Research Paper

GEOSPHERE

GEOSPHERE, v. 16, no. 1

https://doi.org/10.1130/GES02105.1

9 figures; 2 tables; 1 set of supplemental files

CORRESPONDENCE:
vladislav.powerman@gmail.com

CITATION: Powerman, V., Hanson, R., Nosova, A., Girty, G.H., Hourigan, J., and Tretiakov, A., 2020, Nature and timing of Late Devonian–early Mississippian island-arc magmatism in the Northern Sierra terrane and implications for regional Paleozoic plate tectonics: Geosphere, v. 16, no. 1 p. 258–280, https://doi.org/10.1130/GES02105.1.

Science Editor: David E. Fastovsky
Associate Editor: Christopher J. Spencer

Received 15 December 2018
Revision received 22 July 2019
Accepted 30 October 2019

Published online 16 December 2019

Nature and timing of Late Devonian–early Mississippian island-arc magmatism in the Northern Sierra terrane and implications for regional Paleozoic plate tectonics

Vladislav Powerman[1,2], Richard Hanson[3], Anna Nosova[4], Gary H. Girty[5], Jeremy Hourigan[6], and Andrei Tretiakov[7]

[1]Institute of the Earth's Crust, Russian Academy of Science, Irkutsk 664033, Russia
[2]Schmidt Institute of Physics of the Earth, Russian Academy of Sciences, Moscow 123242, Russia
[3]Department of Geological Sciences, Texas Christian University, Fort Worth, Texas 76129, USA
[4]Institute of Geology of Ore Deposits, Petrography, Mineralogy and Geochemistry, Russian Academy of Sciences (IGEM RAS), Moscow 119017, Russia
[5]Department of Geological Sciences, San Diego State University, San Diego, California 92182, USA
[6]Department of Earth & Planetary Sciences, University of California–Santa Cruz, Santa Cruz, California 95064, USA
[7]Geological Institute, Russian Academy of Sciences, Moscow 119017, Russia

ABSTRACT

The Northern Sierra terrane is one of a series of Paleozoic terranes outboard of the western Laurentian margin that contain lithotectonic elements generally considered to have originated in settings far removed from their present relative locations. The Lower to Middle Paleozoic Shoo Fly Complex makes up the oldest rocks in the terrane and consists partly of thrust-imbricated deep-marine sedimentary strata having detrital zircon age signatures consistent with derivation from the northwestern Laurentian margin. The thrust package is structurally overlain by the Sierra City mélange, which formed within a mid-Paleozoic subduction zone and contains tectonic blocks of Ediacaran tonalite and sandstone with Proterozoic to early Paleozoic detrital zircon populations having age spectra pointing to a non–western Laurentian source. Island-arc volcanic rocks of the Upper Devonian Sierra Buttes Formation unconformably overlie the Shoo Fly Complex and are spatially associated with the Bowman Lake batholith, Wolf Creek granite stock, and smaller hypabyssal felsic bodies that intrude the Shoo Fly Complex. Here, we report new results from U-Pb sensitive high-resolution ion microprobe–reverse geometry (SHRIMP-RG) dating of 15 samples of the volcanic and intrusive rocks, along with geochemical studies of the dated units. In addition, we report U-Pb laser ablation–inductively coupled plasma–mass spectrometry ages for 50 detrital zircons from a feldspathic sandstone block in the Sierra City mélange, which yielded abundant Ordovician to Early Devonian (ca. 480–390 Ma) ages. Ten samples from the composite Bowman Lake batholith, which cuts some of the main thrusts in the Shoo Fly Complex, yielded an age range of 371 ± 9 Ma to 353 ± 3 Ma; felsic tuff in the Sierra Buttes Formation yielded an age of 363 ± 7 Ma; and three felsic hypabyssal bodies intruded into the Sierra City mélange yielded ages of 369 ± 4 Ma to 358 ± 3 Ma. These data provide a younger age limit for assembly of the Shoo Fly Complex and indicate that arc magmatism in the Northern Sierra terrane began with a major pulse of Late Devonian (Famennian) igneous activity. The Wolf Creek stock yielded an age of 352 ± 3 Ma, showing that the felsic magmatism extended into the early Mississippian. All of these rocks have similar geochemical features with arc-type trace-element signatures, consistent with the interpretation that they constitute a petrogenetically linked volcano-plutonic system. Field evidence shows that the felsic hypabyssal intrusions in the Sierra City mélange were intruded while parts of it were still unlithified, indicating that a relatively narrow time span separated subduction-related deformation in the Shoo Fly Complex and onset of Late Devonian arc magmatism. Following recent models for Paleozoic terrane assembly in the western Cordillera, we infer that the Shoo Fly Complex together with strata in the Roberts Mountains allochthon in Nevada migrated south along a sinistral transform boundary prior to the onset of arc magmatism in the Northern Sierra terrane. We suggest that the Shoo Fly Complex arrived close to the western Laurentian margin at the same time as the Roberts Mountains allochthon was thrust over the passive margin during the Late Devonian–early Mississippian Antler orogeny. This led to a change in plate kinematics that caused development of a west-facing Late Devonian island arc on the Shoo Fly Complex. Due to slab rollback, the arc front migrated onto parts of the Sierra City mélange that had only recently been incorporated into the accretionary complex. In the mélange, blocks of Ediacaran tonalite, as well as sandstones having detrital zircon populations with non–western Laurentian sources, may have been derived from the Yreka and Trinity terranes in the eastern Klamath Mountains, where similar rock types occur. If so, this suggests that these Klamath terranes were in close proximity to the developing accretionary complex in the Northern Sierra terrane in the Late Devonian.

INTRODUCTION

Passive-margin sedimentation persisted along the western Laurentian margin beginning with late Neoproterozoic rifting until the onset of plate

convergence as recorded by the initiation of arc magmatism and crustal shortening in the region in Middle to Late Devonian time (Rubin et al., 1990; Colpron and Nelson, 2009, 2011). This change in tectonic regime represents the first of a series of orogenic events to affect the evolving continental margin during the formation of the North American Cordillera. Several tectonic terranes occur outboard of the Paleozoic passive margin (Fig. 1), some of which show stratigraphic and faunal linkages with western Laurentia (peri-Laurentian realm in the terminology of Nelson et al., 2013) and are inferred to have initially formed on Laurentian crust in the middle Paleozoic (e.g., Yukon-Tanana, Stikinia, and Quesnellia in Fig. 1). Terranes grouped in the Arctic–NE Pacific realm by Nelson et al. (2013) are exotic with respect to western Laurentia. These terranes are interpreted to have developed in the ancestral northeastern Pacific Ocean (e.g., Wrangellia); evolved as island arcs offshore of northern Laurentia; or contain tectonic elements that show evidence of having originated in the vicinity of Baltica, Siberia, and the northern Caledonide belt prior to arrival in their present positions. The study of these far-traveled terranes—their birthplace, character, and timing of drift with respect to western Laurentia—is essential for understanding the complex tectonic history of the North American Cordillera and also bears on global paleogeographic reconstructions.

The southernmost terrane of the Cordillera that is inferred to contain rocks that originated in the Arctic–NE Pacific realm is the Northern Sierra terrane, which is separated from strata of the Paleozoic passive margin in Nevada by deep-marine Paleozoic strata of the Roberts Mountains and Golconda allochthons (Fig. 1). The stratigraphically lower part of the Northern Sierra terrane consists of the extensive Shoo Fly Complex, which contains a thick, thrust-imbricated package of mostly siliciclastic sedimentary rocks deposited in deep-marine environments, as well as a major mélange unit (Sierra City mélange) that formed in a subduction-zone setting and contains igneous blocks or detrital zircon populations pointing to derivation from the Arctic realm (Girty and Wardlaw, 1984; Harding et al., 2000; Grove et al., 2008). Upper Devonian–lower Mississippian volcanic rocks unconformably overlie the Shoo Fly Complex, and, along with associated intrusive rocks, they record a distinct pulse of mid-Paleozoic island-arc magmatism that many workers have linked to the broadly coeval Antler orogeny along the Paleozoic passive margin to the east. Here, we present comprehensive U-Pb zircon sensitive high-resolution ion microprobe–reverse geometry (SHRIMP-RG) data from volcanic and intrusive units within the Devonian–Mississippian arc, which previously had been dated for the most part by U-Pb isotopic analyses on multigrain zircon fractions from a limited number of samples (e.g., Saleeby et al., 1987; Hanson et al., 1988). We also present additional data from detrital zircons in part of the Sierra City mélange lying a short distance stratigraphically beneath the unconformity with overlying Upper Devonian arc strata. The new data allow timing relations between final stages in the assembly of the Shoo Fly Complex and the onset of Paleozoic arc magmatism in the Northern Sierra terrane to be addressed in detail, which sheds new light on the Paleozoic plate-tectonic evolution of the terrane and its relations to other, broadly coeval parts of the collage of tectonic terranes within the western Cordillera.

REGIONAL TECTONIC FRAMEWORK

During the Devonian, the change from a long-lived passive margin to an active plate boundary along the western Laurentian margin resulted in initiation of Middle to Late Devonian continental volcanic arc magmatism in the parautochthonous Kootenay terrane in southeast British Columbia and in east-central Alaska, along with coeval parts of the Yukon-Tanana, Stikinia, and Quesnellia terranes within the peri-Laurentian realm (e.g., Dusel-Bacon et al., 2006; Paradis et al., 2006; Colpron and Nelson, 2009; Nelson et al., 2013). Arc magmatism continued in the peri-Laurentian terranes after they became detached from the continental margin when the Slide Mountain marginal ocean began opening in Late Devonian–early Mississippian time; remnants of this ancient ocean are preserved in the Slide Mountain terrane (Piercey et al., 2012). Ordovician to Silurian arc magmatism preceded establishment of the Devonian arc in what is now the southern part of the Yukon-Tanana terrane in southeastern Alaska, which was originally located either outboard of the northern part of the terrane or along strike farther to the north, where it may have connected with coeval arc rocks developing in the Arctic realm (Pecha et al., 2016).

Wright and Wyld (2006) proposed that some of the exotic terranes within what is now termed the Arctic–NE Pacific realm by Nelson et al. (2013), including the Alexander terrane, the Yreka and Trinity terranes in the eastern Klamath Mountains, and the Shoo Fly Complex within the Northern Sierra terrane (Fig. 1), initially began to evolve in Neoproterozoic to early Paleozoic time in settings adjacent to the northern or western margins of Gondwana (all directions used herein are in present coordinates) after breakup of the ancient Rodinia supercontinent. Subsequently, the terranes were tectonically transported along the eastern and southern margins of Laurentia by slab rollback in front of a rapidly moving Scotia-type arc system (e.g., Schellart et al., 2007) prior to their Paleozoic or Mesozoic accretion to the western Laurentian margin. As evidence for such a model, Wright and Wyld (2006) cited the presence of Ediacaran to Early Devonian island-arc assemblages in the Alexander, Yreka, and Trinity terranes, as well as ophiolitic assemblages in the latter two terranes, making their early history markedly unlike almost all the terranes known to have originated on or near the western Laurentian margin. Additionally, parts of all three terranes have yielded detrital zircon U-Pb age spectra that include significant numbers of zircon grains with ages of 1.55–1.45 Ga and 0.65–0.55 Ga that do not match known age distributions in Precambrian crustal units in western Laurentia (Wright and Wyld, 2006, and references therein).

Following publication of this innovative model, increasing evidence has instead been advanced to support derivation of these and similar terranes from settings near Baltica, Siberia, and the Caledonide belt. These links were established on the basis of similar distributions of U-Pb detrital zircon ages (Grove et al., 2008; Anfinson et al., 2011; Miller et al., 2011; Beranek et al., 2013; Schermer et al., 2018), paleontological ties (Potter et al., 1990; Soja, 2008; Soja and Antoshkina, 1997; Soja and Krutikov, 2008), similarities in geological history (Colpron and Nelson, 2009; White et al., 2016), and in the case of

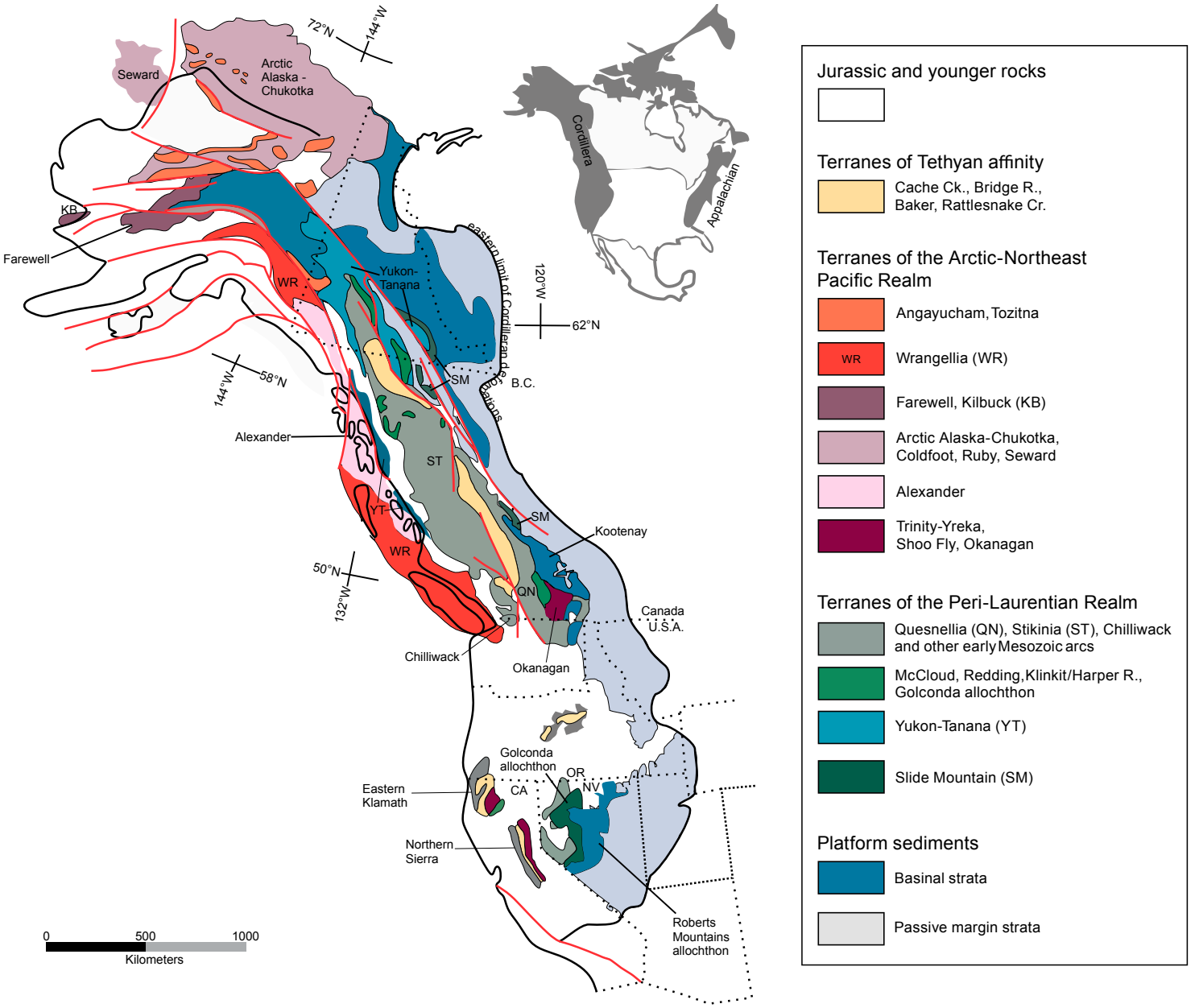

Figure 1. Terranes of the North America Cordillera, modified from Colpron and Nelson (2009) and Nelson et al. (2013). B.C.—British Columbia; OR—Oregon; CA—California; NV—Nevada; Ck—Creek; R—River.

the Alexander terrane, paleomagnetic data (Bazard et al., 1995; Butler et al., 1997). Colpron and Nelson (2009, 2011) proposed that these exotic terranes migrated by slab rollback in a similar manner to that envisioned by Wright and Wyld (2006), but it occurred along the northern Laurentian margin, the so-called "Northwest Passage." In this model, elements of which now appear to be widely accepted, the Alexander, Yreka, and Trinity terranes, as well as parts of the Shoo Fly Complex (the Sierra City mélange), traveled as tectonic fragments that progressively dispersed from each other during westward transport, along with several different terranes in Alaska and the Okanagan terrane in southeast British Columbia (Fig. 1). The Alexander terrane had reached the northwestern corner of Laurentia by Late Devonian–Mississippian time, but the terrane then began a long period of residence, along with Wrangellia, in the ancestral northeast Pacific until Mesozoic accretion against the western Laurentian margin (Colpron and Nelson, 2009, 2011; Nelson et al., 2013). In contrast, after the Yreka, Trinity, and Okanagan terranes and the Sierra City mélange had reached the northwestern corner of Laurentia, they were transported southward along a sinistral transform boundary parallel to the western Laurentian margin. Ordovician–Middle Devonian volcanic arc rocks in the Turtleback and Yellow Aster complexes at the base of the Chilliwack terrane in northern Washington State (Fig. 1; Brown et al., 2010; Schermer et al., 2018) are also inferred to have originated near northern or northeastern Laurentia, but they were emplaced in their present position relative to the western Laurentian margin during Mesozoic strike-slip faulting (Monger et al., 2006; Yokelson et al., 2015; Schermer et al., 2018).

Tectonic interactions between some of the southward-migrating terranes and the western continental margin account for compressional or transpressional deformation documented in places along the margin beginning in Middle Devonian time (e.g., Colpron and Nelson, 2009; Beranek et al., 2016), and farther south in Nevada, this included emplacement of the Roberts Mountains allochthon over the passive margin during the Late Devonian–early Mississippian Antler orogeny (e.g., Dickinson, 2000, 2006). Southward migration of the terranes provided the sources for west-derived clastic sediments with non–western Laurentian detrital zircon signatures that were deposited onto the passive margin beginning in Late Devonian time (Gehrels and Pecha, 2014; Beranek et al., 2016). Colpron and Nelson (2009) suggested that onset of Devonian continental arc magmatism along the western Laurentian margin was driven by east-directed subduction that nucleated along the zone of weakness created by the transform plate boundary. The same authors inferred that the Upper Devonian–Lower Mississippian arc in the Northern Sierra terrane, which is the main subject of this paper, was constructed upon the Shoo Fly Complex after that unit had arrived near the margin farther south. Permian arc rocks and associated strata in the Alexander, Yukon-Tanana, Stikinia, Quesnellia, Chilliwack, and Northern Sierra terranes contain the distinctive McCloud fauna (Miller, 1987). The same fauna also occurs in Permian strata in the eastern Klamath Mountains, which make up part of a succession of Lower Devonian and younger, partly arc-related strata (Redding section) that largely postdate formation of the Yreka and Trinity terranes (Dickinson, 2000; Lindsley-Griffin et al., 2008). The McCloud fauna is considered to have evolved on the order of 2000–3000 km away from the Laurentian margin and generally at more southerly latitudes than the present positions of the terranes containing the fauna (Belasky et al., 2002; Stevens and Belasky, 2009). This evidence indicates that in late Paleozoic times, all these terranes formed a festoon of island arcs outboard of the Slide Mountain ocean, which, after its Late Devonian–early Mississippian initiation, progressively widened by slab rollback as the arcs migrated seaward (Colpron and Nelson, 2009; Piercey et al., 2012). Parts of this ocean extended as far south as the Havallah basin in Nevada, in which Upper Devonian–Permian deep-marine strata accumulated prior to eastward thrusting over the continental margin to form the Golconda allochthon during the Late Permian–Early Triassic Sonoma orogeny (Miller et al., 1984, 1992; Dickinson, 2000, 2006). Most of the other terranes containing the McCloud fauna were likely accreted in the same time frame, although some, such as the Alexander terrane, were not accreted until later in the Mesozoic (Nelson et al., 2013).

GEOLOGICAL SETTING OF THE STUDY AREA IN THE NORTHERN SIERRA TERRANE

Rock units within the Northern Sierra terrane (Fig. 2) show varying degrees of deformation and regional low-grade metamorphism as a result of Middle Jurassic to Cretaceous orogenesis, as well as contact metamorphism associated with emplacement of Jurassic and Cretaceous plutonic rocks (e.g., Hanson et al., 1996; Schweickert, 2015). Original rock types are readily recognizable, however, and we omit the prefix "meta-" for the sake of simplicity. The oldest and laterally most extensive unit in the Northern Sierra terrane is the Lower to Middle Paleozoic Shoo Fly Complex, which extends for a considerable distance to the southeast along strike from the area shown in Figure 2 (Schweickert, 2015) and forms the basement to four separate, mostly arc-related sequences that are typically separated by unconformities and range in age from Late Devonian to Early Cretaceous (Harwood, 1992; Schweickert, 2015). The oldest arc rocks occur primarily within the Upper Devonian to Middle Pennsylvanian Taylorsville sequence and in the partly correlative Lake Tahoe sequence in the southeast part of the area shown in Figure 2 (Harwood, 1992). Permian island-arc tholeiitic and calc-alkaline basaltic to andesitic volcanic and volcaniclastic rocks containing McCloud faunal elements rest unconformably on the Taylorsville sequence (Brooks and Coles, 1980; Rouer et al., 1988; Harwood, 1992). The Permian arc rocks are unconformably overlain by Upper Triassic to Cretaceous volcanic and sedimentary strata that are stratigraphically linked to continental-margin volcanic arc rocks resting on Laurentian basement farther east and south, thus tying the Northern Sierra terrane to North America by the Late Triassic.

The Shoo Fly Complex and overlying Upper Devonian to Jurassic arc strata in the southern part of the area shown in Figure 2 have been tilted uniformly to the east. Hanson et al. (1996) interpreted the tilting to have occurred in the Middle Jurassic, although, more recently, Schweickert (2015) has argued that

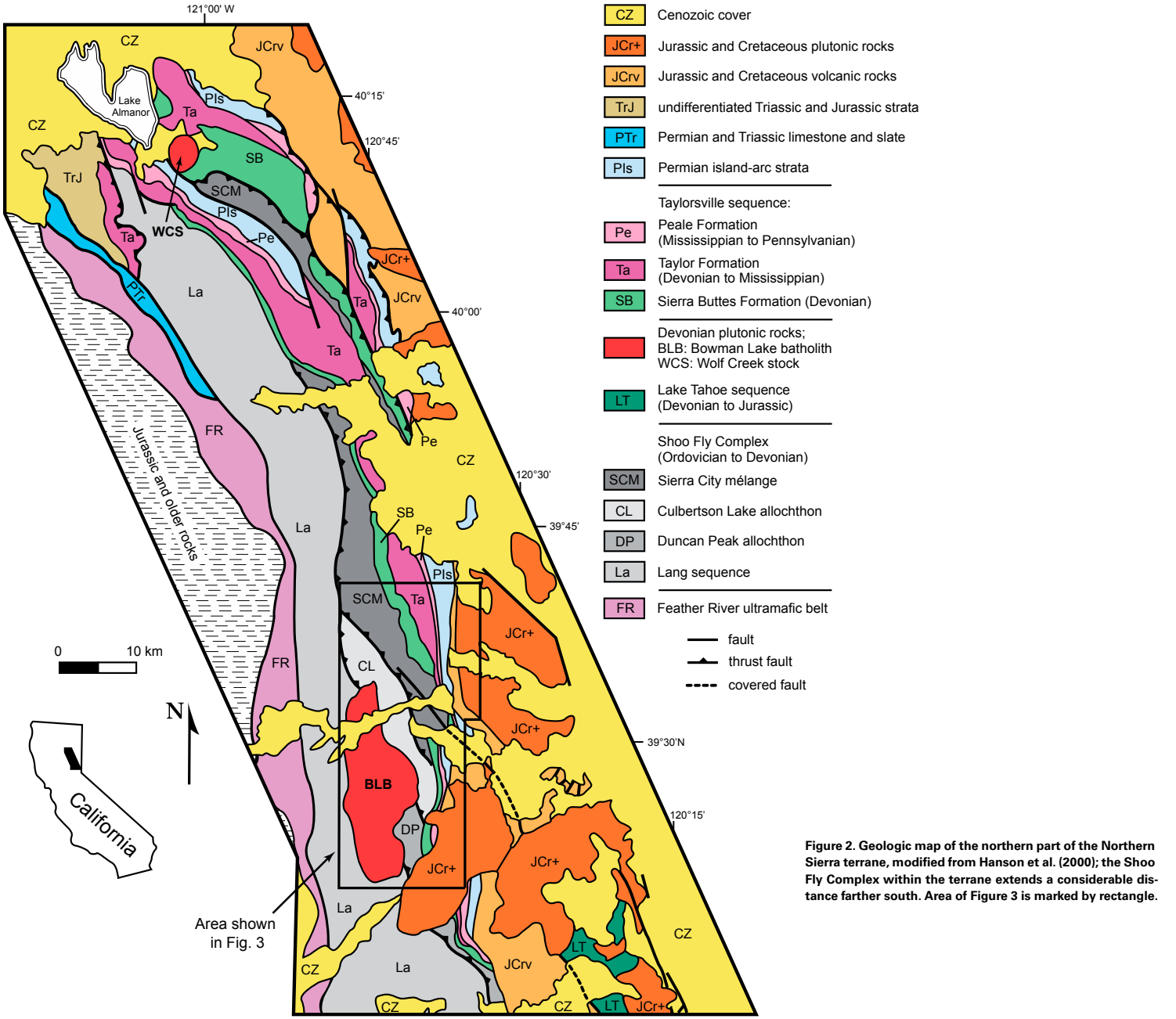

Figure 2. Geologic map of the northern part of the Northern Sierra terrane, modified from Hanson et al. (2000); the Shoo Fly Complex within the terrane extends a considerable distance farther south. Area of Figure 3 is marked by rectangle.

it occurred in the Early Cretaceous. In any case, because of this tilting, the map pattern in the southern part of Figure 2 essentially represents a cross-sectional view of Paleozoic to Middle Jurassic strata exposed between the Feather River ultramafic belt and Mesozoic plutons to the east. Next, we describe the Shoo Fly Complex and the Taylorsville sequence and associated intrusive rocks in more detail, as they are the main focus of this paper.

Shoo Fly Complex

In the area of interest (Fig. 3; see Supplemental Item 3[1] for detailed ArcGIS files for the digital map), the Shoo Fly Complex consists of four large, west-vergent thrust sheets, and it is in structural contact with the Feather River ultramafic belt, a polyphase suture zone separating the Northern Sierra terrane from Paleozoic and Mesozoic oceanic and island-arc terranes to the west (e.g., Saleeby et al., 1989; Schweickert, 2015). The Lang sequence and the Duncan Peak and Culbertson Lake allochthons consist dominantly of Ordovician to pre–Upper Devonian deep-marine siliciclastic and hemipelagic deposits deformed by west-verging tight to isoclinal folds (Schweickert et al., 1984; Girty et al., 1990, 1996; Harwood, 1992). These largely coherent units are structurally overlain by the Sierra City mélange, which is inferred to have formed in an active subduction complex and contains blocks of a variety of rock types set within a matrix of sheared mudstone, sandstone, or serpentinite (Schweickert et al., 1984; Girty and Pardini, 1987; Mount and Schweickert, 1986; Mount, 1990). Sparse tonalite blocks are also present, one of which has yielded a multigrain U-Pb zircon upper-intercept date of 612 ± 29 Ma (Saleeby, 1990; Grove et al., 2008). The mélange is inferred to have undergone mixing by both olistostromal and tectonic-shearing processes within an active subduction complex, and Girty and Pardini (1987) and Mount (1990) provided evidence that sandstone and mudstone were incorporated into the mélange and partly disrupted while the sediments were still unlithified.

Detrital zircons in sandstone turbidites in the lower three, largely intact allochthons within the Shoo Fly Complex have U-Pb age spectra that closely match age populations for northwest Laurentia (Harding et al., 2000; Colpron and Nelson, 2009). Sandstone blocks in the Sierra City mélange, in contrast, have yielded detrital zircon populations that include abundant Neoproterozoic and Silurian to Early Devonian grains, along with grains showing a wide range of older Proterozoic ages that do not match age distributions expected for western or northwestern Laurentia (Girty and Wardlaw, 1984; Harding et al., 2000). Using the laser ablation–inductively coupled plasma–mass spectrometry (LA-ICP-MS) technique, Grove et al. (2008) obtained two main age peaks at ca. 430 Ma and 410 Ma for zircon grains from the same sandstone block studied by Girty and Wardlaw (1984), who analyzed multigrain zircon fractions. Zircon grains from a second sandstone block analyzed by Harding et al. (2000) and Grove et al. (2008) yielded abundant Neoproterozoic ages. These data led Colpron and Nelson (2009) to include the Sierra City mélange as one of the terranes originally derived from the vicinity of Siberia, Baltica, and the northeast Caledonide belt. Grove et al. (2008) also obtained U-Pb dates ranging from 381 ± 9 Ma to 359 ± 11 Ma for four zircon grains from another sandstone block that was analyzed by Girty and Wardlaw (1984), but these analyses are statistical outliers compared to the majority of the data, and their significance is unclear.

Taylorsville Sequence

The basal unit of the Taylorsville sequence is the laterally discontinuous Grizzly Formation, which contains Frasnian and Famennian fossils and overlies the Shoo Fly Complex along a pronounced angular unconformity (Schweickert and Girty, 1981; Hanson and Schweickert, 1986). Terrigenous clastic rocks in the Grizzly Formation were derived primarily from erosion of Shoo Fly rocks, and Girty et al. (1991) presented evidence for deposition of the unit in an active trench-slope-basin setting that was still undergoing deformation during final stages of assembly of the Shoo Fly Complex.

The Sierra Buttes Formation rests conformably on the Grizzly Formation and records the onset of arc magmatism in the Northern Sierra terrane (d'Allura et al., 1977; Harwood, 1992). The unit includes andesitic and felsic subaqueous ash-fall tuff, felsic lava, volcaniclastic turbidites, and coarser subaqueous mass-flow deposits (some of which are rich in pumice) intercalated with black siliceous mudstone and radiolarian chert that contain mid-Famennian ammonoids and conodonts (Anderson et al., 1974; Hannah and Moores, 1986; Hanson and Schweickert, 1986; Brooks, 2000; Silva et al., 2000). Hypabyssal intrusions primarily ranging in composition from basaltic andesite to rhyolite are common and show abundant evidence of interaction with wet, unconsolidated sediments beneath the seafloor, including the common presence of intrusive pillows or zones of peperite (e.g., Hanson and Schweickert, 1982, 1986; Hanson, 1991). Previously published geochemistry indicates that these rocks are dominantly calc-alkaline in composition (Rouer et al., 1989; Brooks, 2000; Silva et al., 2000). Rouer et al. (1989) and Silva et al. (2000) reported epsilon Nd values for the felsic rocks ranging from –0.1 to –19.6, and the latter authors inferred that these low values reflect various degrees of interaction between mantle-derived arc magmas and continentally derived siliciclastic detritus in the Shoo Fly Complex.

The Sierra Buttes Formation is conformably overlain by island-arc tholeiitic to calc-alkaline basaltic to andesitic volcanic rocks of the Taylor Formation (Rouer et al., 1989; Harwood, 1992; Brooks, 2000), which in turn is conformably overlain by the discontinuous lower member of the Peale Formation. The latter unit is characterized by basaltic, latitic, and rhyolitic volcanic and volcaniclastic rocks belonging to the shoshonitic series (Rouer et al., 1989), which record the last stage of arc magmatism in the Taylorsville sequence and contain early Mississippian (Kinderhookian) fossils (Harwood, 1992). These rocks are overlain by a distinctive unit, the upper Peale Formation, which consists mostly of rhythmically bedded radiolarian chert that can be traced throughout the part of the Northern Sierra terrane shown in Figure 2. Fossil radiolaria indicate slow sedimentation over a long time interval from the late early Mississippian to at

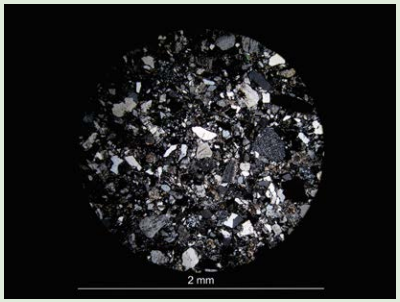

[1]Supplemental Items. Item 1: Figure S1. Thin section image of the volcanic sandstone (wacke) from the block in the Sierra City mélange, polarizers crossed. Item 2: Volcanic sandstone (wacke) sample from the Sierra City mélange thin section description. Item 3: ArcGIS files for the digitized geologic map of the Bowman Lake and Sierra Buttes vicinity. Item 4: Table of sensitive high-resolution ion microprobe–reverse geometry (SHRIMP-RG) analytical U-Th-Pb data for zircons from magmatic rocks of the Northern Sierra terrane. Item 5: Laser-ablation–inductively coupled plasma–mass spectrometry (LA-ICP-MS) analytical U-Th-Pb data for detrital zircons from the sandstone sample, Sierra City mélange. Please visit https://doi.org/10.1130/GES02105.S1 or access the full-text article on www.gsapubs.org to view the Supplemental Items.

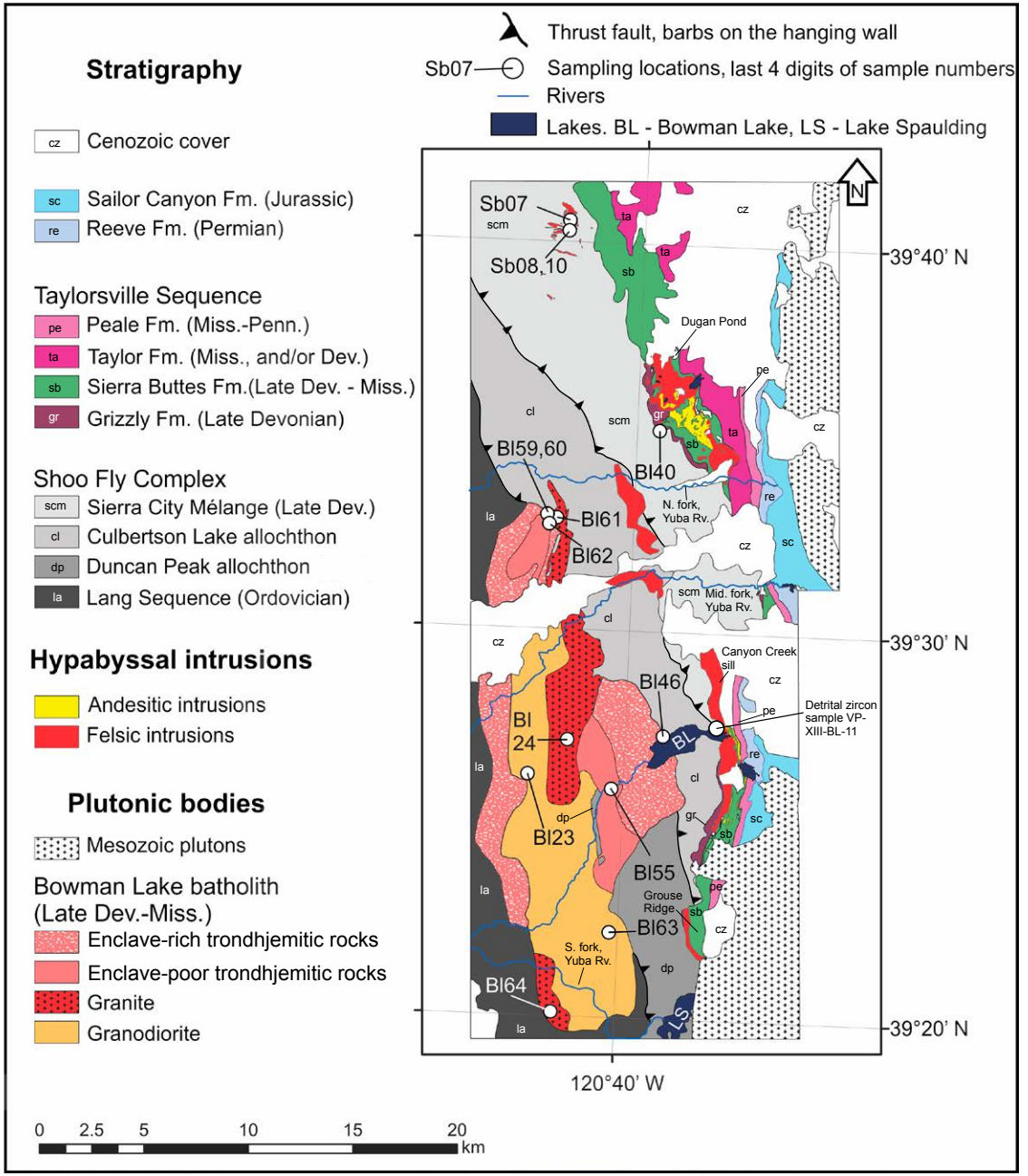

Figure 3. Compiled geologic map of the Bowman Lake batholith area. Mapping sources include Mount (1990); Saucedo and Wagner (1992); Hanson and Schweickert (1986); Hanson et al. (1988); and unpublished field maps of R.E. Hanson and G.H. Girty. ArcGIS project files for this map are provided with the Supplemental Items (see text footnote 1).

least the middle Pennsylvanian, although the younger age range for the unit is uncertain because it is overlain disconformably by Permian (late Wolfcampian) island-arc strata (Harwood, 1992).

Middle Paleozoic Plutonic Rocks

Two shallow-level plutonic bodies in the Northern Sierra terrane in the area shown in Figure 2 are considered to be directly related to the volcanic and hypabyssal intrusive rocks in the Sierra Buttes Formation. The Wolf Creek biotite granite stock, with an area of ~20 km^2, intrudes the Sierra City mélange and Sierra Buttes Formation in the northern part of the terrane (Saleeby et al., 1987). The larger, composite Bowman Lake batholith occurs ~90 km to the south-southeast, extends ~25 km in a north-south direction, and is as much as 10 km across (Fig. 3). It is broadly concordant with regional structural trends in the Shoo Fly Complex but cuts discordantly across some of the structural panels and major thrust faults within that unit. The following description of the batholith is mostly condensed from Hanson (1983) and Hanson et al. (1988).

Tonalitic and trondhjemitic rocks form significant parts of the batholith in its northern part and along its eastern and western margins. Hanson et al. (1988) divided these rocks into an inclusion-rich and an inclusion-poor facies, but here we refer to these units as enclave-rich and enclave-poor facies, in accordance with more widely used terminology (Barbarin, 2005). The enclave-rich facies contains abundant ovoid enclaves of biotite-hornblende tonalite (Fig. 4H) and less common hornblende gabbro <4 m long set within a trondhjemite and trondhjemitic tonalite host containing biotite and hornblende in significantly smaller amounts. Enclaves in the enclave-poor facies are petrographically identical to those in the enclave-rich facies but are smaller and present in much lower amounts. The enclaves in many cases show fluidal cuspate margins against the more felsic host rocks and in some cases also show chilled margins, supporting the interpretation that the enclaves represent blobs of gabbroic to tonalitic magma that mingled with cooler, more felsic magma during emplacement of these parts of the batholith (e.g., Blake et al., 1965; Bacon, 1986; Frost and Mahood, 1987; Barbarin, 2005). Biotite-hornblende granodiorite makes up much of the middle portion of the batholith, and biotite granite crops out in three separate areas, although the two northern areas are likely to be continuous beneath Cenozoic cover.

Numerous dacitic to rhyolitic hypabyssal intrusions penetrate the batholith, the Shoo Fly Complex, and the Grizzly Formation to the east (Fig. 3 and 4A–4C). They petrographically closely resemble the felsic hypabyssal intrusions that occur at slightly higher stratigraphic levels and were emplaced during or shortly after deposition of Sierra Buttes sedimentary strata. Most of the hypabyssal intrusions penetrating the batholith and the Shoo Fly Complex are too small to depict on the scale of Figure 3, but the larger ones in the Shoo Fly Complex in part contain trondhjemite and biotite granite of the same types that make up major parts of the batholith. Based on these field relations and the U-Pb zircon geochronological data available at the time, Hanson et al. (1988) interpreted the Bowman Lake batholith, associated hypabyssal intrusions, and the Sierra Buttes Formation to represent an island-arc volcano-plutonic complex exposed in cross section due to the large-scale eastward tilting that affected this part of the Northern Sierra terrane. Significantly, detailed mapping of some of the dacitic to rhyolitic intrusions in the Sierra City mélange in the northern part of the area depicted in Figure 3 has shown that the intrusions have well-developed peperite along contacts against sedimentary material within the mélange matrix; these relations indicate that at least parts of the matrix were still unlithified and rich in pore water at the time the felsic magmatism was occurring (Mount, 1990).

Previous Geochronology

Previous geochronological studies of Late Devonian magmatism in the Northern Sierra terrane relied primarily upon the thermal ionization mass spectrometry (TIMS) method applied to multigrain zircon fractions. These data yielded ages of 409 ± 16 Ma for granite in the Bowman Lake batholith (Girty et al., 1984) and 378 +5/–10 Ma for the Wolf Creek stock (Saleeby et al., 1987). Subsequent analyses of multigrain zircon fractions from samples of trondhjemite, granodiorite, and granite from the Bowman Lake batholith and the Canyon Creek sill within the Sierra Buttes Formation reported by Hanson et al. (1988) revealed complex isotopic systematics reflecting multiple discordance mechanisms, leading to a model U-Pb age for the batholith between Ma 385 and 364 Ma. Based on these results, Hanson et al. (1988) argued that the ca. 409 Ma result of Girty et al. (1984) reflected inheritance of older Pb. More recently, analyses of zircons following acid-leaching experiments, again using the TIMS multigrain technique, resulted in an age of 369 ± 3 Ma for granodiorite from the batholith (Hanson et al., 1996), although the analytical data were not published. Finally, Cecil et al. (2012) obtained an age of 372 ± 6 Ma for zircon from granite within the batholith using the LA-ICP-MS technique, as part of a study on Mesozoic granitoid plutonism in the northern Sierras.

SAMPLING AND ANALYTICAL METHODS

Sample Description

To develop better geochronological constraints on the timing of middle Paleozoic arc magmatism in the Northern Sierra terrane, 10 samples were collected along three transects through the Bowman Lake batholith (Fig. 3; Table 1), along with one sample from the Wolf Creek stock from the same location sampled by Saleeby et al. (1987); three samples of hypabyssal felsic intrusions studied by Mount (1990) north of the Bowman Lake batholith (Fig. 3) that show peperitic margins against adjacent parts of the Sierra City mélange; one sample from a felsic hypabyssal intrusion spatially associated with the Wolf Creek stock; and one sample from a felsic ash-fall tuff located in

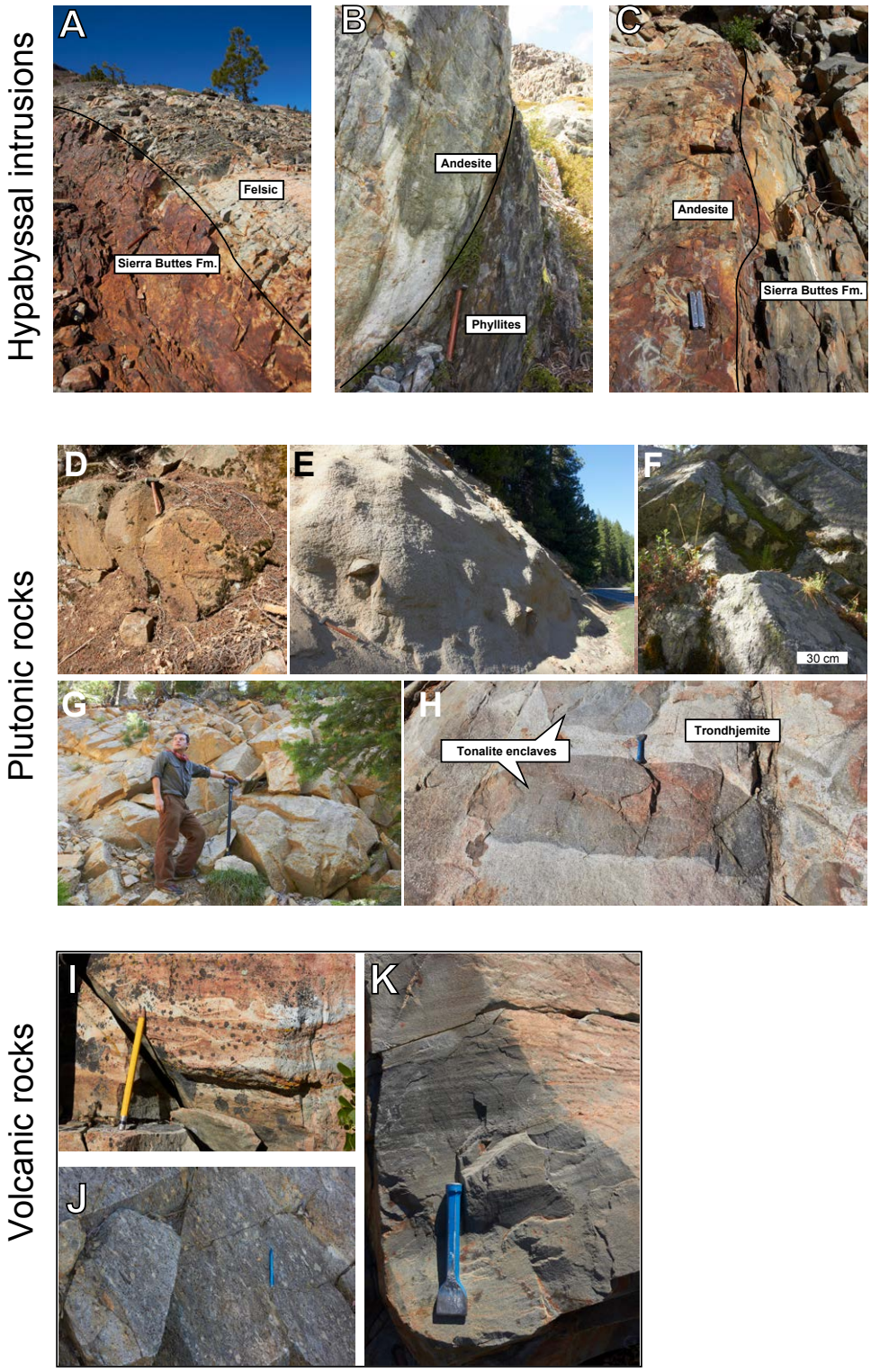

Figure 4. Photographs of selected igneous outcrops. (A–C) Intrusive contacts of hypabyssal bodies against volcaniclastic deposits in the Sierra Buttes Formation (A, C) and against phyllite in the Sierra City mélange (B). (D–H) Plutonic rocks showing granite in Bowman Lake batholith (D), granite in Wolf Creek stock (E), enclave-poor facies in Bowman Lake batholith (F), granodiorite in Bowman Lake batholith (G), and enclave-rich facies in Bowman Lake batholith (H). (I–K) Volcaniclastic rocks in the Sierra Buttes Formation.

TABLE 1. GEOGRAPHICAL LOCATIONS, UNITS, AND SUMMARIZED GEOCHRONOLOGY RESULTS OF THE ANALYZED SAMPLES

Sample no.	Lat. (°N)	Long. (°W)	Lithology	Comments	Age (Ma) (95% conf)	XRF data?§
Bowman Lake batholith (BLB)						
VP-XIII-BL-11	39°27.688′	120°37.070′	Feldspathic sandstone		Detrital zircons (see text)	No
VP-XI-BL-23	39°26.238′	120°43.158′	Granodiorite	Middle transect	368 ± 8	Yes
VP-XI-BL-24	39°27.166′	120°41.912′	Granite	"	370 ± 6	No
VP-XI-BL-46	39°27.271′	120°38.646′	Trondhjemite, ERF*	"	364 ± 5	Yes
VP-XI-BL-55	39°25.980′	120°40.474′	Trondhjemite, EPF†	"	358 ± 6	"
VP-XI-BL-59	39°33.008′	120°42.713′	Trondhjemite, ERF*	Northern transect	357 ± 6	"
VP-XI-BL-60	39°33.008′	120°42.713′	Mafic enclave	"	353 ± 3	"
VP-XI-BL-61	39°32.918′	120°42.536′	Granite	"	371 ± 9	"
VP-XI-BL-62	39°32.729′	120°42.762′	Trondhjemite, EPF†	"	360 ± 7	"
VP-XI-BL-63	39°22.197′	120°40.257′	Granodiorite	Southern transect	362 ± 4	"
VP-XI-BL-64	39°20.127′	120°42.102′	Granite	"	367 ± 4	No
					Weighted average for BLB only = 361 ± 5 Ma (95% conf.), MSWD# = 7.4	
Wolf Creek stock						
VP-XII-SB-03					352 ± 3	Yes
VP-XII-SB-05	40°10.508′	121°01.485′	Granite	Wolf Creek stock	No geochronology	"
Hypabyssal intrusions						
VP-XII-SB-01	39°27.478′	120°36.758′	Quartz porphyry	Canyon Creek sill near Bowman Lake	No geochronology	Yes
VP-XII-SB-02	40°10.522′	120°59.293′	Quartz porphyry	Hypabyssal intrusion near Wolf Creek stock	"	"
VP-XII-SB-07	39°40.190′	120°42.543′	Quartz porphyry	Felsic dike intruding Sierra City mélange	358 ± 3	"
VP-XII-SB-08	39°40.245′	120°42.477′	Dacite	"	367 ± 3	"
VP-XII-SB-09	39°40.297′	120°42.447′	Basaltic andesite	"	No geochronology	"
VP-XII-SB-10	39°40.388′	120°42.428′	Quartz porphyry	"	369 ± 4	"
VP-XII-SB-24	39°38.848′	120°42.270′	"	"	No geochronology	"
VP-XI-BL-32	39°36.535′	120°39.388′	"	Small felsic intrusion	"	"
VP-XI-BL-33	39°36.804′	120°39.325′	"	Quartz-rich hypabyssal intrusion	"	"
VP-XI-BL-47	39°27.421′	120°36.341′	Andesite	Andesitic sill with large plagioclase phenocrysts	"	"
Sierra Buttes Formation						
VP-XI-BL-40	39°35.409′	120°39.142′	Thinly bedded siliceous tuff	Member A (lower part of the formation)	363 ± 9	No
					Weighted average for entire igneous system = 361 ± 4 Ma (95% conf.)	

*ERF—enclave-rich facies.
†EPF—enclave-poor facies.
§XRF—X-ray fluorescence.
#MSWD—mean square of weighted deviation.

the lower part of the Sierra Buttes Formation on the southwest side of Sierra Buttes (Fig. 3), which comes from member A of that unit as defined by Hanson and Schweickert (1986). In order to augment data published by Grove et al. (2008), we also collected a sample from a block of feldspathic volcaniclastic sandstone (wacke) from the Sierra City mélange for detrital zircon analysis (thin section image of this sample along with its lithological description can be found in Supplemental Items 1 and 2 [footnote 1]).

Geochemical data for the Bowman Lake batholith and Wolf Creek stock have not previously been published, and only limited amounts of major- and trace-element data are available from the Sierra Buttes Formation and related hypabyssal intrusions in the area of Figure 3. In order to better document the nature of Late Devonian magmatism in the Northern Sierra terrane, we present new geochemical results for most of the samples collected for geochronology. Low-grade metamorphism in the Bowman Lake batholith and Wolf Creek stock is recorded by partial to complete replacement of biotite and hornblende by chlorite, actinolite, titanite, and epidote-group minerals. Similar mineral assemblages typically completely replace mafic phenocrysts and groundmass phases in the mafic to felsic hypabyssal intrusions related to the Sierra Buttes Formation. Orthoclase and microperthite in the plutonic rocks generally show only slight alteration to sericite, but plagioclase in all the rocks is heavily altered to sericite, calcite, and epidote-group minerals (Hanson, 1983; Saleeby et al., 1987; Hanson et al., 1988). These petrographic observations indicate that the major oxides in the rocks are likely to have been disturbed to various degrees, particularly the highly mobile elements like the alkalis (e.g., Rollinson, 1993). We therefore place greater emphasis on the more immobile elements (e.g., Th, Nb, Zr, Ti, Y, etc.) in considering the geochemical data.

U-Pb Zircon Geochronology

Igneous Zircons: SHRIMP-RG Dating

All zircon U-Pb measurements from igneous samples were carried out in the Stanford-U.S. Geological Survey (USGS) SHRIMP-RG laboratory. Zircons were separated using standard crushing, sizing, hydrodynamic, magnetic, and density methods. Zircons chosen for analysis were hand selected using a binocular microscope and screened for suitability on the basis of cathodoluminescence imaging. Generally, the zircons were transparent and exhibited well-developed euhedral prismatic and pyramidal morphologies.

Zircon crystals were mounted in epoxy, ground, polished, ultrasonically cleaned, and Au coated. Sputter pits produced with an ~5 nA O_2^- primary beam were ~25 µm in diameter. U and Th concentrations were standardized with "Madagascar" zircon ($^{207}Pb/^{206}Pb$ = 550 Ma; 4196 ppm U, 1166 ppm Th; Barth and Wooden, 2010). Calibration of Pb/U ratios was performed using R33 zircon ($^{206}Pb/^{238}U$ = 419 Ma; Black et al., 2004; Mattinson, 2010) as the primary standard. In some instances (see Supplemental Item 4 [footnote 1]), we also used zircons from the Duluth Gabbro complex (AS3, 1099 Ma; Paces and Miller, 1993) to independently assess the precision and accuracy of the ion probe U-Pb analyses. Data were reduced using the SQUID plug-in for Excel (Ludwig, 2009). Ages for geological interpretations were calculated using the $^{206}Pb/^{238}U$ isotopic ratio; $^{207}Pb/^{206}Pb$ ratios were not used due to the absence of old (Precambrian) grains. Discordance was calculated between $^{206}Pb/^{238}U$ and $^{207}Pb/^{235}U$ ages. The mean square weighted deviation (MSWD) for each sample was compared against the critical MSWD value versus degrees of freedom (table 1 *in* Mahon, 1996) to assess the scatter at 95% confidence. We interpreted MSWD values higher than the critical value to indicate that geological factors in the sense of Schoene (2014) contributed to the observed scatter; otherwise, the scatter was interpreted to have been caused by analytical uncertainties alone. Complete geochronological data tables for the samples are provided in Supplemental Item 4.

Detrital Zircons: LA-ICP-MS Dating

Detrital zircons were analyzed at the University of California–Santa Cruz using a Photon Machines Analyte 193 nm excimer laser equipped with a Helex 2-volume ablation cell, coupled with a single-collector Thermo Element XR magnetic sector ICP-MS. A single zircon spot analysis consisted of 30 s of baseline data collection, followed by 30 s of on-peak data collection, during which the laser was continuously pulsed at a 10 Hz rate, with energy stabilized laser fluence of 4.0 J cm^{-2}. Laser firing was followed by 20 s of delay before the next analysis. The usual spot size was 34 µm. Sometimes, we chose a narrower beam when dealing with very small zircons. Series of four primary (R33) and secondary (AS3 or FC3) analyses were run at the beginning and end of each session. During the session, the primary analyses were run each fifth sample, and secondary analyses were run each tenth sample. The ablated and aerosolized zircon was exported from the ablation cell through 4 mm (outer diameter) Teflon tubing by helium gas mixed with argon sample gas, and then injected into an inductively coupled plasma stream. The ATLEX 300i laser was energy stabilized at 4.5 mJ. Downstream, a user-settable beam attenuator provided energy density control. The Element XR was operated in electrostatic mode, allowing rapid peak-hopping within the following range of collected ions: ^{202}Hg: 15 ms, $^{204}(Pb + Hg)$: 15 ms, ^{206}Pb: 15 ms, ^{207}Pb: 30 ms, ^{208}Pb: 15 ms, ^{232}Th: 3 ms, ^{235}U: 6 ms, and ^{238}U: 3 ms. A single run cycle took 120 ms, with 102 ms of this being on-peak, while the remainder represented total dead time during peak hops between ions.

Data reduction was performed using Iolite software, version 2.31 (Paton et al., 2011). The external uncertainties were estimated by multiplying the internal (measurement) uncertainties by the square root of MSWD of the standard zircons. We used the exponential detrending algorithm based on the downhole fractionation of standards, resizing the integration periods in cases of drill-throughs and spikes of ^{204}Pb.

Further data filtering of reduced data was done with Dezirteer software (www.dezirteer.com; Powerman et al., 2018). The following filters were used:

positive discordance (+20%), negative discordance (–10%), age uncertainties (>10%). Discordance was calculated between $^{206}Pb/^{238}U$ and $^{207}Pb/^{235}U$ and between $^{206}Pb/^{238}U$ and $^{207}Pb/^{206}Pb$ ages; the smallest of the two values was used during the filtering. The "best" age of a grain was calculated from either $^{206}Pb/^{238}U$ or $^{207}Pb/^{206}Pb$, depending on the lower uncertainty between the two systems. Analytical geochronological data for the detrital zircons are provided in Supplemental Item 5 (footnote 1).

Geochemistry

Major and trace elements were analyzed at San Diego State University by X-ray fluorescence (XRF) for most samples collected for geochronology except volcaniclastic deposits in the Sierra Buttes Formation. Samples for major-element analysis were prepared using an HD Elektroniks VAA2 automatic fuser with platinum crucibles and molds for the fused glass discs. Samples were fused with lithium tetraborate as a flux, with a flux:sample ratio of 6:1. Trace elements were analyzed on pressed powder pellets prepared using a Spex Press (model 3264B) with a 40 mm die assembly. Sample powders were mixed with an "Elvacite" binder, i.e., a mixture of 200 g Elvacite per liter of acetone. Pressed pellets used 2 mL of binder for 13 g of sample. Pellets were pressed to 25 tons. Analyses were done using a Philips Magix Pro wavelength dispersive sequential X-ray spectrometer system equipped with a 4 kW light element supersharp Rh target end window X-ray tube. Additionally, this system included: close-coupled optics for maximum signal strength, a full set of analyzer crystals for the analysis of elements in the range of O-U, three detectors (a flow and a sealed proportional detector in tandem plus a scintillation detector in parallel), a range of beam filters and collimators, vacuum operation for the analysis of solids, helium environment for liquids and loose powders, a 4 kW/125 mA solid-state X-ray generator, and an automatic sample changer set up to handle 36 samples. The Philips Magix Pro system utilizes the Philips SuperQ Data Collection and Evaluation Software, v4. USGS and Canadian rock standards were used for calibration. Ausmon was used as a monitor with all runs.

RESULTS

Geochronology

Igneous Samples: SHRIMP-RG Dating

U-Pb zircon isotopic ages for the analyzed igneous samples are summarized in Table 1 and Figures 5 and 6; the detailed analytical data are reported in Supplemental Item 4 (footnote 1). The majority of analyses did not reveal any significant Pb loss. In several instances, we analyzed both the cores and rims of zircons to check for possible inheritance; none was found in our sample suite.

Bowman Lake batholith. Samples from the Bowman Lake batholith yielded mean weighted $^{238}U/^{206}Pb$ dates ranging from 371 ± 9 Ma to 353 ± 3 Ma (MSWD = 7.4) (Table 1; Figs. 5 and 6). Analytical results are given in Supplemental Item 4; here, we review the results for each analyzed sample.

One granodiorite sample (VP-XI-BL-23) from the middle transect through the batholith (Table 1; Fig. 3) yielded zircon ages ranging from 382 ± 7 Ma to 350 ± 7 Ma (n = 10). The weighted mean age is 368 ± 8 Ma, with an MSWD of 2.2, which exceeds the MSWDcrit (critical mean square weighted deviation value, corresponding to the degree of freedom = 9 from table 1 in Mahon, 1996) value of 2.1. A second granodiorite sample (VP-XI-BL-63) from the southern transect contained zircons with ages from 382 ± 10 Ma to 338 ± 9 Ma (n = 24). The weighted mean age is 362 ± 4 Ma, with an MSWD of 1.4, which is less than the MSWDcrit value of 1.7.

One granite sample (VP-XI-BL-64) from the southern transect contained zircons yielding ages from 383 ± 10 Ma to 337 ± 9 Ma (n = 28). The weighted mean age is 367 ± 4 Ma, with an MSWD of 1.2, which is less than the MSWDcrit value of 1.6. Another granite sample (VP-XI-BL-24) from the middle transect contained zircons with an age range of 384 ± 7 Ma to 347 ± 6 Ma (n = 13). The weighted mean age is 370 ± 6 Ma, with an MSWD of 2.0, exceeding the MSWDcrit value of 1.9. A final granite sample (VP-XI-BL-61) from the northern transect yielded zircons with ages ranging from 386 ± 13 Ma to 356 ± 14 Ma (n = 9). The weighted mean age is 371 ± 9, with an MSWD of 0.7, which is less than the MSWDcrit value of 2.1.

An enclave-rich trondhjemite sample (VP-XI-BL-46) from the middle transect yielded zircons with ages ranging from 377 ± 7 Ma to 353 ± 7 Ma (n = 8), with a weighted mean age of 364 ± 5 Ma and an MSWD of 1.6, which is less than the MSWDcrit value of 2.3. Another enclave-rich trondhjemite sample (VP-XI-BL-59) from the northern transect yielded zircons with ages ranging from 386 ± 10 Ma to 333 ± 6 Ma (n = 19), with a weighted mean age of 357 ± 6 Ma and an MSWD of 3.3, which is greater than the MSWDcrit value of 1.75. A mafic enclave sample (VP-XI-BL-60), collected at the same location as trondhjemite sample VP-XI-BL-59 discussed above, yielded zircons with ages ranging from 371 ± 7 Ma to 335 ± 7 Ma (n = 22), with a weighted mean age of 353 ± 3 Ma and an MSWD of 1.6, which is less than the MSWDcrit value of 1.7; note that this result is within error of the age for the host trondhjemite.

An enclave-poor trondhjemite (VP-XI-BL-55) from the middle transect yielded zircons with ages ranging from 376 ± 10 Ma to 348 ± 9 Ma, with a weighted mean age of 358 ± 6 Ma and an MSWD of 0.6, which is less than the MSWDcrit value of 2.1. Another enclave-poor trondhjemite (VP-XI-BL-62) from the northern transect yielded zircons with ages ranging from 378 ± 10 Ma to 330 ± 8 Ma (n = 25), with a mean weighted age of 360 ± 7 Ma and an MSWD of 2.9, which is greater than the MSWDcrit value of 1.6.

Hypabyssal intrusions in the Sierra City mélange. Three felsic intrusions hosted in the Sierra City mélange were analyzed. Sample VP-XII-SB-07 yielded zircons with ages ranging from 369 ± 6 Ma to 353 ± 4 Ma (n = 10) with a mean weighted age of 358 ± 3 Ma and an MSWD of 0.9, which is less than MSWDcrit value of 2.1. A second intrusion (sample VP-XII-SB-08) yielded zircons with

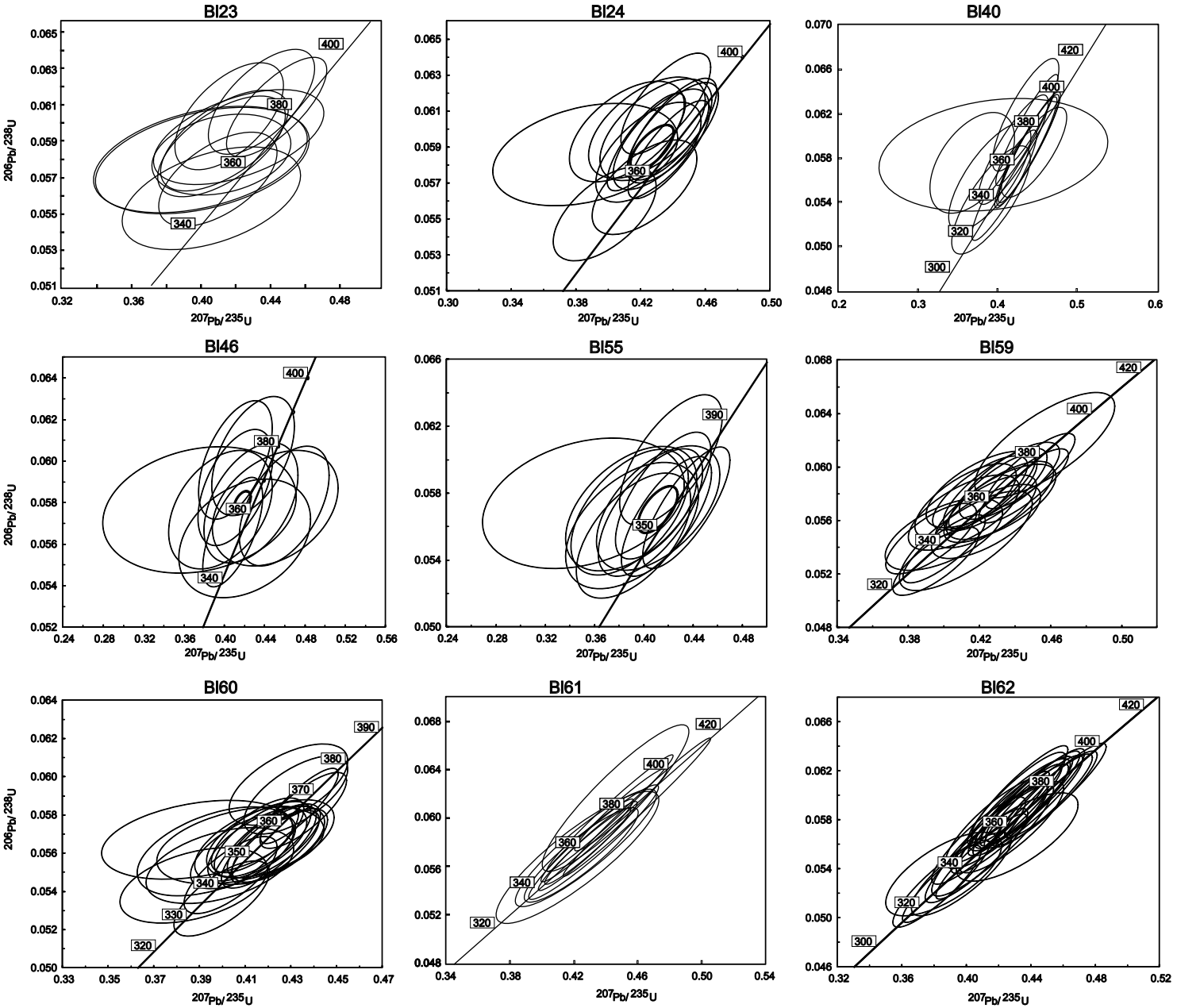

Figure 5. Conventional concordia diagrams. Results are shown at 2σ. (***Continued on following page.***)

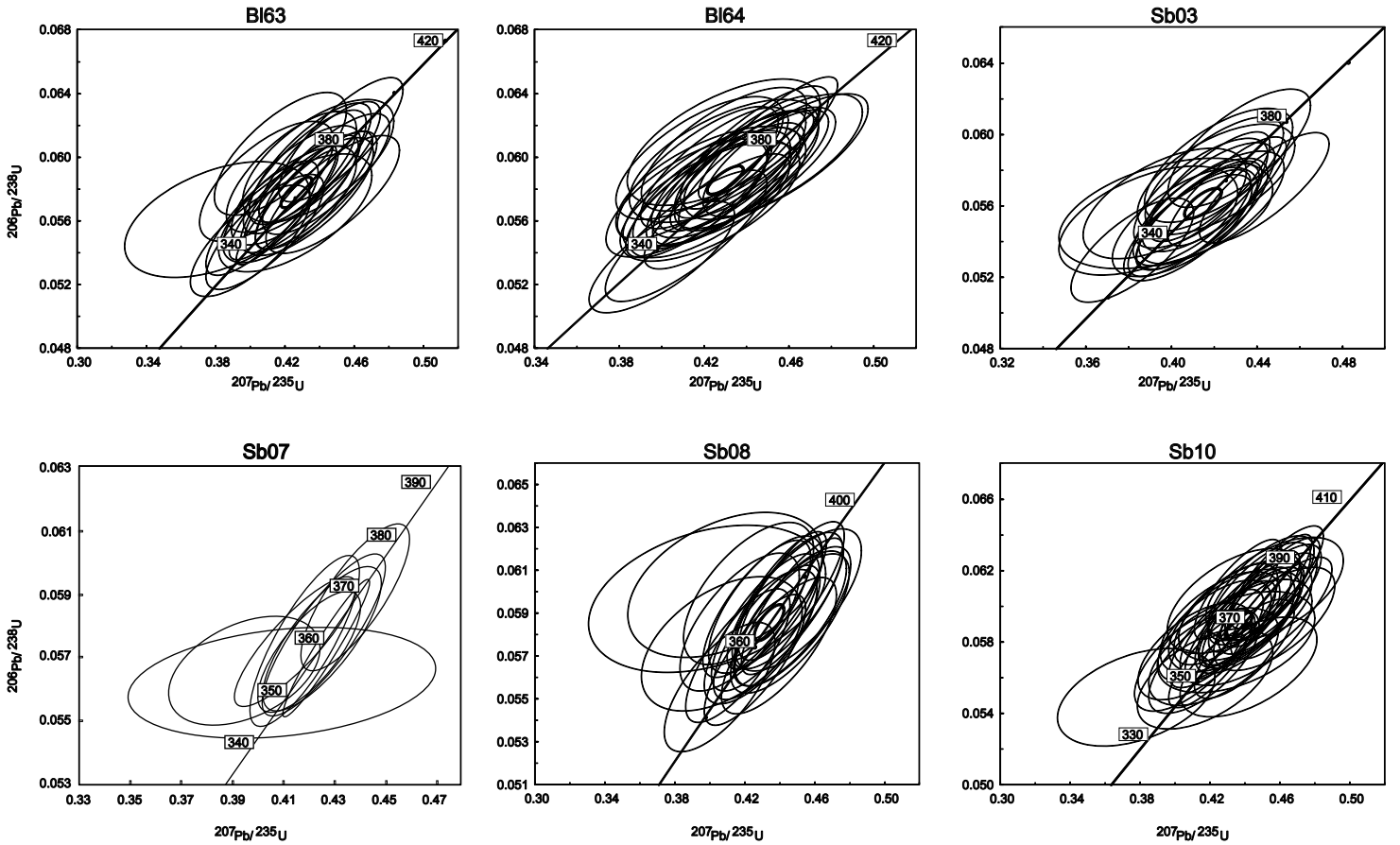

Figure 5 (*continued*).

ages ranging from 378 ± 8 Ma to 349 ± 8 Ma (n = 22) with a mean weighted age of 367 ± 3 Ma and an MSWD of 0.9, which is less than the MSWDcrit value of 1.7. The final intrusion analyzed (sample VP-XII-SB-10) yielded zircons with ages ranging from 386 ± 7 Ma to 345 ± 7 Ma (n = 35) with a mean weighted age of 369 ± 4 Ma and an MSWD of 2.1, which exceeds MSWDcrit value of 1.5.

Sierra Buttes Formation. The only geochronological sample analyzed for this unit (VP-XI-BL-40) was a subaqueous felsic ash-fall tuff, which yielded zircons with ages ranging from 387 ± 12 Ma to 338 ± 12 Ma (n = 12); the mean weighted age is 363 ± 9 Ma, with an MSWD of 1.3, which is less than the MSWDcrit value of 2.0.

Wolf Creek granite stock. A single sample VP-XII-SB-03 was analyzed for this pluton and yielded zircons with ages ranging from 371 ± 8 Ma to 336 ± 7 Ma (n = 20); the mean weighted age is 352 ± 3 Ma, with an MSWD of 1.1, which is less than the MSWDcrit value of 1.7.

Detrital Sample: LA-ICP-MS Dating

Detrital zircon analytical data for sample VP-XII-BL-11 from volcaniclastic sandstone in the Sierra City mélange yielded 51 analyses after reduction in

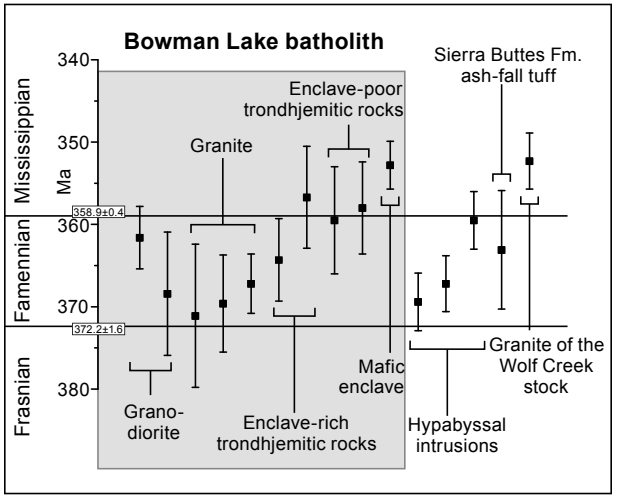

Figure 6. Summary of acquired U-Pb zircon ages for all samples. Bars represent 2σ uncertainties. Beginning and end of Famennian Stage are after Gradstein and Ogg (2012).

lolite, and 50 of these passed further data filtering and were used for geologic interpretations. Analytical results are given in Supplemental Item 5 (footnote 1). While the "best" ages lie in the 1955–370 Ma range, the population is almost unimodal (Fig. 7), with the majority of ages forming a spectrum from Early Ordovician to Late Devonian, and with only three Precambrian zircons (Fig. 7, bottom left). The following peaks were recognized using Dezirteer's algorithm, which finds peaks on a probability density plot: 375 Ma (8%), 393 Ma (24%), 418 Ma (52%), 482 Ma (4%), 1086 Ma (4%), 1620 Ma (4%), and 1955 Ma (4%). The definition of age peaks greatly depends on the type of probability diagram used. Kernel density estimates plotted with bandwidth = 13 Ma, for example, result in recognition of a sole Phanerozoic peak at 420 Ma. Using the "unmix ages" routine in Isoplot (plug-in for MS-Excel; Ludwig, 2003) on only the portion of grains that are Phanerozoic in age, we calculated the following peaks: 381 Ma (20%), 409 Ma (26%), 422 Ma (24%), 433 Ma (26%), 452 Ma (3%), and 482 Ma (2%).

Geochemistry

Major- and trace-element data are reported in Table 2. The major-element data are shown on standard diagrams in Figures 8A, 8B, and 8C in order to illustrate the overall compositional range of the plutonic and hypabyssal intrusive rocks, although, as noted in the Shoo Fly Complex section of the geologic setting section earlier herein, care is needed in interpreting these data because of the metamorphic overprint. The analyzed rocks plot primarily as granitoids (Fig. 8A), and they are magnesian (Mg# = 0.22–0.43; Fig. 8B) and calc-alkalic in composition, with modified alkali-lime index (MALI) values of 5.9–7.9 (Frost et al., 2001). Most samples are weakly to moderately peraluminous (A/CNK = 1.0–1.36, where A/CNK = $Al_2O_3/[CaO + Na_2O + K_2O]$; Fig. 8C; Shand, 1943), but the range in aluminum saturation index (ASI) probably at least partly reflects loss or gain of alkalis during low-grade metamorphism.

Because of the secondary overprint, in Figure 8 we also plot the samples in the Winchester and Floyd (1977) classification diagram (Fig. 8D), the Nb versus Y diagram of Pearce et al. (1984) (Fig. 8E), and the Ti versus Zr discrimination diagram of Pearce (1982) (Fig. 8F), which employ immobile elements that are resistant to alteration. Also shown in these figures are published data from basaltic to rhyolitic volcanic and hypabyssal intrusive rocks in the Sierra Buttes Formation from Rouer et al. (1989) and Silva et al. (2000). We recognize that the diagrams of Winchester and Floyd (1977) and Pearce (1982) were designed for use with volcanic rocks, but for comparison purposes, we show data from the Bowman Lake batholith and Wolf Creek stock on these diagrams as well. The data overall indicate that the plutonic rocks exhibit a similar range in chemical composition to the Sierra Buttes volcanic and hypabyssal rocks, supporting the interpretation that these various units are in general part of a single, petrogenetically linked magmatic system. This is emphasized for the felsic rock samples in the Nb versus Y diagram, where the data are tightly clustered in the field for volcanic arc and syncollisional granites. In the Ti versus Zr diagram of Pearce (1982), almost all the data fall in the volcanic arc field, except for a few basaltic to andesitic sills in the Sierra Buttes Formation, which may reflect some contribution from a different source region. Detailed consideration of the petrogenesis of the Late Devonian–early Mississippian arc rocks in the Northern Sierra terrane is beyond the scope of the present study but is clearly an important avenue for future research.

DISCUSSION AND CONCLUSIONS

Late Devonian–Early Mississippian Evolution of the Northern Sierra Terrane

U-Pb ages for the Bowman Lake batholith, spatially associated felsic hypabyssal intrusions, and tuff in the Sierra Buttes Formation in general overlap within error (Fig. 6). The results support the interpretation of Hanson et al. (1988) that these various volcanic and intrusive units are components of a linked volcano-plutonic magmatic system, but they provide better age resolution than the U-Pb dates derived from multigrain zircon fractions. Using the time scale of Gradstein and Ogg (2012), the results are also generally consistent with the presence of mid-Famennian fossils within the Sierra Buttes Formation (Fig. 9), but they indicate that emplacement of parts of the volcano-plutonic assemblage continued into the early Mississippian. Our new U-Pb age of 352 ± 3 Ma for the Wolf Creek stock to the north is significantly younger than the

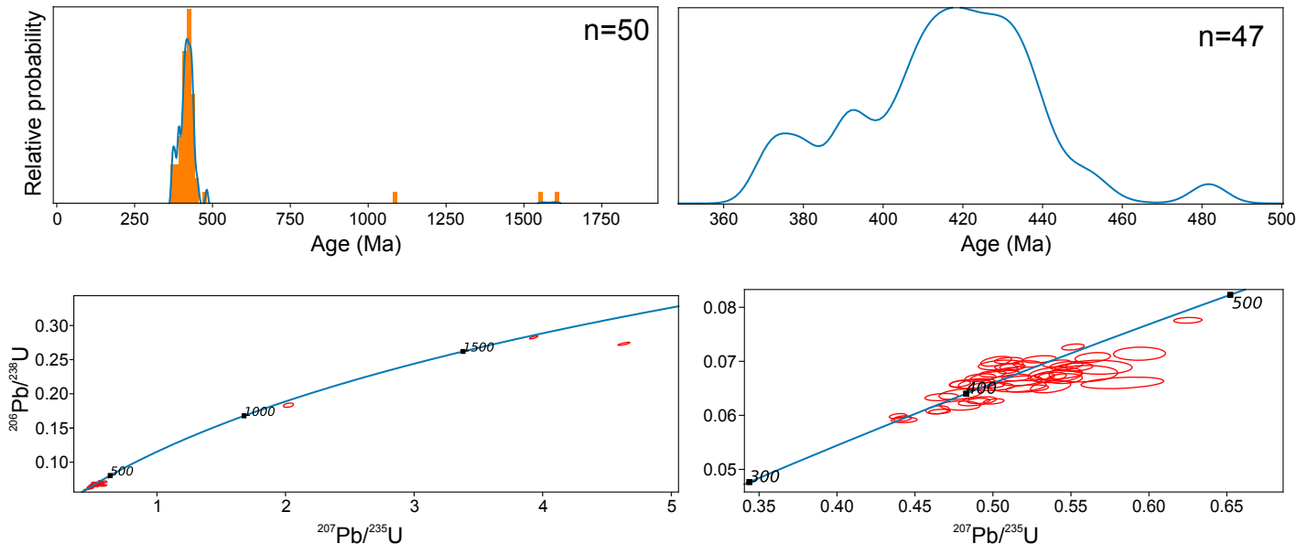

Figure 7. Summary of acquired U-Pb detrital zircon ages for sample VP-XIII-BL-11. Top row: Probability density plots for the entire spectrum (left, also includes histogram) and for interval younger than 500 Ma (right). Bottom row: Conventional concordia diagrams, full range (left) and for interval younger than 500 Ma (right).

TABLE 2. RESULTS OF THE X-RAY FLUORESCENCE GEOCHEMISTRY

Sample no.	Rock type	Geochronology done?	Trace elements (ppm)																					Major elements (wt%)									
			Sc	V	Cr	Co	Ni	Cu	Zn	Rb	Sr	Y	Zr	Nb	Cs	Ba	La	Ce	Nd	Sm	Hf	Pb	Th	U	SiO_2	Al_2O_3	Fe_2O_3	CaO	MgO	K_2O	Na_2O	MnO	TiO_2	P_2O_5	Total
VP-XI-BL-23	Granodiorite, middle transect	Yes	11	44	5	14	<5	5	46	49	115	25	104	5.7	<1	502	5.8	11.9	2.1	5.2	2.6	5.1	4.3	3.7	72.5	14.0	3.47	3.86	0.64	1.80	3.10	0.061	0.273	0.039	99.76
VP-XI-BL-32	Quartz porphyry	No	8	12	7	9	<5	6	18	49	67	31	119	5.8	<1	1378	<5	<5	<1	3.0	3.0	4.2	5.0	5.1	77.5	12.5	1.91	0.19	0.48	2.84	3.49	0.016	0.113	0.019	99.05
VP-XI-BL-33	"	"	19	16	17	16	<5	3	49	37	77	30	112	4.5	<1	536	<5	8.4	1.2	3.9	2.8	<1	3.3	4.1	72.5	12.9	4.36	1.16	0.62	2.32	3.05	0.038	0.304	0.061	97.37
VP-XI-BL-46	IRF*, middle transect	Yes	8	32	8	12	<5	5	10	49	206	21	117	6.8	<1	960	<5	<5	<1	3.1	2.9	1.6	2.5	3.1	73.7	13.8	2.69	3.23	0.58	2.46	2.72	0.026	0.217	0.033	99.49
VP-XI-BL-47	Andesitic sill	No	34	296	39	39	19	134	96	48	332	19	73	3.5	2.4	2452	40.3	84.9	37.4	<1	1.9	30.0	11.1	7.6	53.5	18.2	10.18	4.85	3.99	2.76	4.67	0.115	0.669	0.289	99.25
VP-XI-BL-55	IPF†, middle transect	Yes	12	61	12	16	<5	8	42	58	146	24	114	7.4	<1	557	<5	16.1	3.6	2.8	2.8	2.2	3.9	3.3	71.1	14.1	4.11	2.97	0.95	1.77	3.15	0.075	0.305	0.044	98.64
VP-XI-BL-59	IRF*, northern transect	"	13	87	5	19	<5	6	26	32	196	16	41	2.6	<1	316	<5	<5	<1	3.2	1.2	<1	<2	1.4	71.7	12.6	4.81	3.18	2.42	1.19	2.20	0.054	0.44	0.077	98.64
VP-XI-BL-60	Mafic inclusion in IRF*, northern transect	"	52	227	75	43	16	310	82	18	287	18	29	2.0	<1	198	<5	10.4	22.9	4.3	<1	2.2	<2	1.0	50.0	16.0	11.02	9.85	6.76	0.64	1.95	0.191	0.395	0.049	96.88
VP-XI-BL-61	Granite, northern transect	"	5	9	7	9	<5	4	4	31	64	27	99	7.4	<1	173	5.7	<5	<1	2.6	2.5	1.2	11.3	3.8	77.5	12.7	1.31	0.14	0.49	0.95	5.20	0.01	0.11	0.016	98.48
VP-XI-BL-62	IPF†, northern transect	"	22	129	14	22	6	5	31	3	311	19	60	4.1	<1	116	<5	15.4	4.4	3.3	1.6	<1	<2	1.3	66.6	13.9	5.40	6.65	2.06	0.17	2.89	0.082	0.345	0.046	98.22
VP-XI-BL-63	Granodiorite, northern transect	"	6	24	4	13	<5	7	36	99	110	28	132	7.3	<1	655	15.3	24.6	7.7	4.6	3.3	8.7	9.1	5.5	73.4	13.4	2.77	2.46	0.48	2.78	3.16	0.05	0.229	0.037	98.72
VP-XII-SB-01	Canyon Creek sill	No	17	36	4	15	<5	12	40	<1	61	25	146	8.2	<1	42	7.7	25.0	6.6	5.7	3.6	7.6	8.4	4.5	71.4	15.0	4.07	0.44	1.24	0.06	7.48	0.033	0.287	0.044	100.10
VP-XII-SB-02	Quartz porphyry near Wolf Creek stock	"	9	<2	6	14	<5	3	20	6	85	40	130	6.9	<1	183	<5	<5	<1	4.6	3.2	<1	3.2	2.5	78.7	11.1	3.26	1.52	0.59	0.41	4.55	0.028	0.189	0.025	100.38
VP-XII-SB-03	Wolf Creek Stock granite	Yes	6	25	6	14	<5	51	24	111	252	22	119	7.6	<1	1008	12.4	24.2	6.2	4.1	2.9	14.0	7.4	5.3	72.0	14.0	2.90	2.05	0.50	3.45	2.82	0.038	0.205	0.048	97.96
VP-XII-SB-05	"	No	5	25	11	19	<5	37	46	119	214	21	127	6.6	<1	1128	14.1	17.6	4.0	2.6	3.1	37.5	10.4	6.8	72.2	13.4	2.90	2.06	0.60	3.78	2.86	0.043	0.173	0.039	98.06
VP-XII-SB-07	Quartz porphyry	Yes	17	60	13	23	<5	4	10	8	129	22	97	3.4	1.0	85	<5	13.8	2.7	3.8	2.4	3.4	2.1	3.4	71.2	13.0	5.98	1.81	1.75	0.32	4.43	0.05	0.382	0.055	99.01
VP-XII-SB-08	Quartz porphyry	"	25	108	6	26	<5	4	16	18	103	20	80	3.4	1.3	248	<5	21.3	6.1	4.3	2.1	<1	<2	2.8	67.0	13.0	6.97	2.69	2.43	0.73	3.50	0.076	0.462	0.066	96.95
VP-XII-SB-09	Basaltic andesite hypabyssal	No	24	333	56	40	44	251	111	43	327	24	82	4.9	2.8	1246	16.1	44.4	35.5	4.7	2.0	11.0	<2	2.9	51.0	15.4	10.99	5.82	4.37	1.33	3.86	0.18	0.949	0.485	94.36
VP-XII-SB-10	Quartz porphyry	Yes	21	115	4	23	<5	4	11	21	78	21	88	3.5	<1	265	<5	16.0	3.9	4.9	2.2	<1	2.3	3.4	70.7	13.1	5.82	1.55	1.92	0.77	4.11	0.051	0.404	0.047	98.47
VP-XII-SB-24	"	No	9	6	4	8	<5	34	6	10	43	24	107	4.1	<1	44	<5	<5	<1	4.4	2.7	1.1	4.5	3.4	76.6	13.0	2.00	0.10	0.34	0.31	6.59	0.016	0.188	0.047	99.21

Note: Selected chemical analyses of the observed rock types. Major elements are in wt%, and trace elements are in ppm.
*Trondhjemite, IRF—inclusion-rich facies.
†Trondhjemite, IPF—inclusion-poor facies.

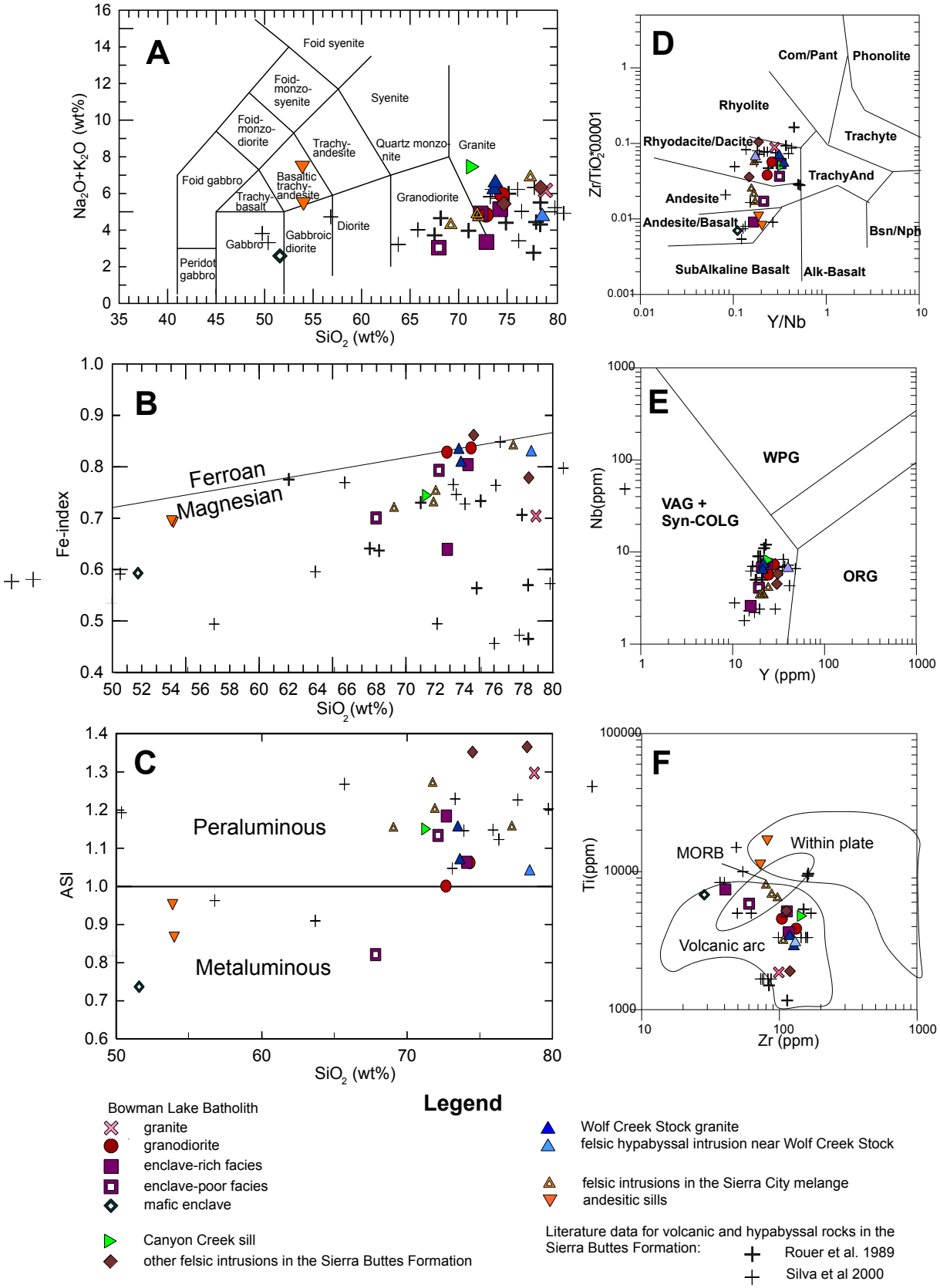

Figure 8. Geochemical results. (A) Total alkali vs. silica (TAS) diagram for igneous rock classification (Middlemost, 1994). (B) Fe-index = (FeO + 0.9Fe_2O_3)/(FeO + 0.9Fe_2O_3 + MgO) against the SiO_2 content with the ferroan and magnesian rock fields after Frost and Frost (2008). (C) ASI (aluminum saturation index = Al/[Ca – 1.67P + Na + K]) vs. SiO_2, after Shand (1943). (D) Zr/TiO_2–Y/Nb classification diagram after Winchester and Floyd (1977). And—andesite; Bas—basanite; Com—comendite; Pant—pantellerite; Nph—nephelinite; Alk—alkaline. (E) Nb-Y discriminant diagram for syncollision (syn-COLG), volcanic arc (VAG), within-plate (WPG), and normal and anomalous ocean-ridge (ORG) granites, after Pearce et al. (1984). (F) Ti-Zr discrimination diagram, after Pearce (1982). MORB—mid-ocean-ridge basalt.

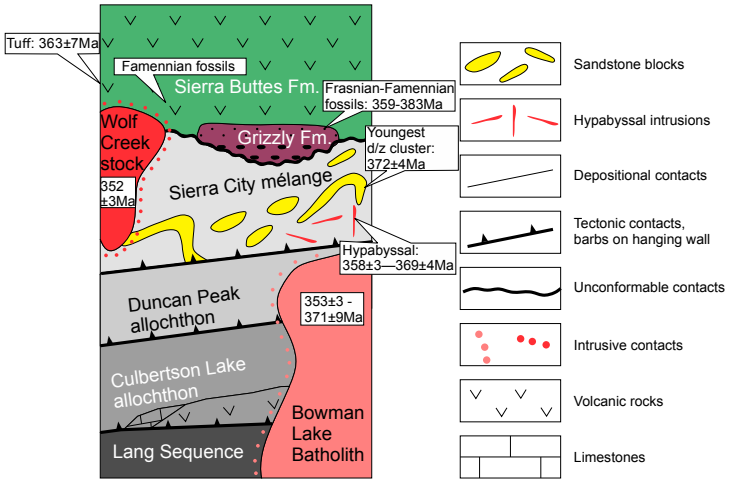

Figure 9. Age constraints plotted on a schematic section showing composite relationships for Shoo Fly Complex and overlying Grizzly and Sierra Buttes Formations, modified after Saleeby et al. (1987). Sources: hypabyssal intrusions, Bowman Lake batholith, Wolf Creek stock, Sierra Buttes Formation—this study; youngest detrital zircon cluster in the Sierra City mélange—sample VP-XIII-BL-11 from this study; Frasnian–Famennian fauna in Grizzly Formation—Hanson and Schweickert (1986). Abbreviation: d/z—detrital zircon.

previously available ca. 378 Ma date for this pluton based on multigrain zircon fractions (Saleeby et al., 1987), which, as noted by those authors, appear to contain a component of inherited Proterozoic zircon derived from the Shoo Fly Complex. The new data yield an early Mississippian age for the Wolf Creek stock, possibly close to the end of the Kinderhookian Stage (in North American stratigraphic terminology) at ca. 352 Ma (Gradstein and Ogg, 2012). The age of that chronostratigraphic boundary is, however, not precisely known because of the lack of high-precision isotopic ages for the relevant time frame (Gradstein and Ogg, 2012, p. 627).

Our new ages for different phases of the Bowman Lake batholith range from 371 ± 9 Ma to 353 ± 3 Ma (Table 1). Although minor Pb loss or inheritance not resolvable by the SHRIMP-RG method may have contributed a small amount to the dispersion in measured ages, we interpret the 371–353 Ma age range between the samples to primarily reflect emplacement of the batholith over a significant length of time. Hanson et al. (1988) inferred that the crude concentric zonation shown by the Bowman Lake batholith resulted from successive injection of the main phases into an expanding, high-level magma chamber. In this interpretation, the tonalitic-trondhjemitic magmas rimming the western, northern, and eastern margins of the batholith were emplaced first, followed by intrusion of granodiorite, which breached the marginal tonalitic-trondhjemitic rocks to the south. Granite was emplaced last, partly in the central part of the batholith and partly along zones of weakness on the pluton margins. However, intrusive contacts between the main phases either are not exposed or are ambiguous. The above interpretation was based on then-prevailing views regarding the emplacement of concentrically zoned granitoid plutons (e.g., Bateman and Chappell, 1979).

The new geochronological data show this interpretation to be incorrect and instead indicate that intrusion of the main parts of the batholith overlapped in time (at least within the resolution of SHRIMP-RG data; more precise isotope-dilution TIMS data might indicate otherwise), with the granite and granodiorite partly predating intrusion of the tonalitic-trondhjemitic rocks. Such a model is consistent with a wealth of recent work showing that composite, batholith-scale plutons in volcanic arc settings are typically assembled incrementally from relatively small batches of magma over time spans of millions of years (e.g., Coleman et al., 2004; Glazner et al., 2004; Davis et al., 2012; Frazer et al., 2014; Menand et al., 2015; Shea et al., 2016). The overall geometry of the tilted Bowman Lake batholith (Fig. 3) suggests that it was assembled primarily from sill-like magma injections, although initial upward transport of the magma likely occurred via dikes (e.g., Petford et al., 2000). We interpret the large tabular mass of Shoo Fly rock between the central granodiorite and the trondhjemitic-tonalitic rocks to the east (Fig. 3) to represent a screen that separated these different parts of the batholith during incremental assembly. Mappable tabular Shoo Fly masses near and along the contact between granite and enclave-rich trondhjemitic-tonalitic rocks in the northern part of the batholith (Fig. 3) represent a similar, partly disrupted screen.

Because the Bowman Lake batholith cuts the three lower allochthons of the Shoo Fly Complex, the oldest zircon age of 371 ± 9 Ma for different phases of the batholith provides a minimum age for juxtaposition of these allochthons. Emplacement of the Sierra City mélange at the structural top of the Shoo Fly Complex must have occurred prior to 369 ± 4 Ma, which is the oldest mean weighted age we obtained for hypabyssal felsic bodies that intrude the mélange (Fig. 6). As noted above, these hypabyssal felsic intrusions show field evidence that they were emplaced prior to lithification of the mélange matrix (Mount, 1990). Together with evidence that Upper Devonian strata in the Grizzly Formation (Fig. 9) accumulated in an active trench-slope-basin setting (Girty et al., 1991), these data indicate that a relatively narrow time interval separated final stages of assembly of the Shoo Fly Complex and Late Devonian arc magmatism in the Northern Sierra terrane. This in turn implies an abrupt shift in the location of the active volcanic arc, and a simple explanation for this would be slab rollback, causing the arc front to migrate onto parts of its accretionary complex.

Our new detrital zircon analyses for a sandstone block within the mélange reveal an age distribution dominated by Ordovician to Early Devonian grains, which is similar to results from one of the sandstone blocks analyzed by Grove et al. (2008). Our sample also yielded three zircon analyses with a weighted mean age of 372 ± 4 Ma, suggesting comparison with the four zircon grains analyzed by Grove et al. (2008) from the other sandstone block they studied that yielded ages of 381 ± 9 Ma to 359 ± 11 Ma. These results are consistent with Late Devonian deposition of sandstone making up some of the blocks within the mélange, which would be in accord with other evidence showing

that onset of Late Devonian arc magmatism in the Northern Sierra terrane in the study area only slightly postdated formation of at least parts of the mélange. More precise analyses (e.g., chemical-abrasion isotope-dilution TIMS) of these relatively young zircons are needed to adequately address this issue.

We infer that as the Late Devonian arc front shifted onto that part of the Shoo Fly Complex, uprising arc magma had difficulty penetrating through this thick package of dominantly low-density sedimentary material due to buoyancy constraints. Initial batches of magma stalled at depth and underwent fractionation coupled with varying amounts of assimilation in magma reservoirs below the present level of exposure. This process resulted in a high proportion of felsic relative to mafic and intermediate rock in the Sierra Buttes Formation and associated subvolcanic plutons, in comparison to most of the younger Paleozoic arc rocks in the Northern Sierra terrane. Such a model is consistent with low initial Nd isotopic ratios in some Sierra Buttes felsic rocks (Rouer et al., 1989; Silva et al., 2000). Tholeiitic to calc-alkaline basalts and andesites in the slightly younger Taylor Formation (Rouer et al., 1989; Brooks, 2000) record a shift to more typical island-arc magma compositions.

Broader Tectonic Implications

Prior to the models proposed by Wright and Wyld (2006) and Colpron and Nelson (2009, 2011), the Late Devonian–early Mississippian arc in the Northern Sierra terrane was considered to have developed on top of the Shoo Fly Complex when the terrane lay west of the passive margin in Nevada, with the arc playing an important role in driving Late Devonian to early Mississippian east-vergent thrusting of deep-marine Cambrian to Middle Devonian strata in the Roberts Mountains allochthon over the passive margin during the Antler orogeny. This event was inferred to record (1) back-arc thrusting behind a west-facing arc; (2) compressional deformation linked to encroachment of an east-facing arc; or (3) some combination of both, such as a flip in subduction polarity (e.g., Schweickert and Snyder, 1981; Miller et al., 1984, 1992; Burchfiel and Royden, 1991; Dickinson, 2000). Our new geochronological data confirm that Late Devonian–early Mississippian arc magmatism in the Northern Sierra overlapped in time with the Antler orogeny, but increasing evidence for southward transport of Paleozoic terranes outboard of a transform boundary along the western Laurentian margin requires reevaluation of traditional models for the Antler event.

Colpron and Nelson (2009) argued that the Sierra City mélange formed during early Paleozoic subduction within the Arctic realm and then became one of the terranes caught up within the subduction system that migrated westward in the middle Paleozoic through the "Northwest Passage" along the northern Laurentian margin. During its westward migration, the terrane was tectonically juxtaposed with the rocks making up the lower three structural panels in the Shoo Fly Complex, which contain detrital zircon age spectra consistent with a northwest Laurentian provenance (Harding et al., 2000). Transport of the resulting composite terrane along the sinistral transform boundary parallel to the western Laurentia margin brought the terrane to a position off the passive margin in Nevada in time for it to serve as basement upon which the Late Devonian–early Mississippian northern Sierran arc was built.

More recently, Linde et al. (2016, 2017) used detrital zircon geochronology and sandstone textural and compositional features of strata within the Roberts Mountains allochthon to argue that most of the units within the allochthon were also deposited well to the north along the western Laurentian margin, in this case, in the vicinity of the Peace River arch in Alberta; these rocks were subsequently tectonically transported to the south along the transform boundary, culminating in transpressional emplacement of the Roberts Mountains allochthon over the passive margin in Nevada. Such a model is supported by evidence that Antler-equivalent strata in Idaho were deposited in a pull-apart basin linked to a sinistral fault regime (Beranek et al., 2016).

Based on this work and building on the model of Colpron and Nelson (2009), we suggest that rocks within the lower three structural panels within the Shoo Fly Complex were transported southward along a strike-slip fault that was outboard of the Roberts Mountains allochthon but was part of the same transform plate boundary. Arrival of these terranes against the northeast-southwest–trending embayment in the passive margin in central Nevada (Fig. 1) blocked farther southward tectonic transport and initiated transpressional deformation along the margin. This must have begun in Frasnian time, as indicated by depositional patterns of strata in the Antler foredeep basin and associated backbulge and forebulge regions, and it was followed by Famennian–early Mississippian emplacement of the Roberts Mountains allochthon on top of the passive margin (Goebel, 1991; Dickinson, 2000, 2006). There is no direct evidence, however, that the Shoo Fly Complex was thrust onto the passive margin, suggesting that it arrived in a position close to the margin but did not collide with it.

We infer that blocking of these southward-migrating terranes against the passive margin caused a rearrangement of the local plate-kinematic framework, leading to initiation of the west-facing northern Sierran arc, which was constructed on parts of the Shoo Fly Complex. Slab rollback led to back-arc extension behind the arc, which began to form the Havallah basin, while transpressional emplacement of the Roberts Mountains allochthon over the passive margin continued farther inboard. This model is supported by the fact that initial stages of the development of the Havallah basin coincided with Late Devonian magmatism in the northern Sierra arc, as shown by the presence of Famennian fossils both in the Sierra Buttes Formation (Hanson and Schweickert, 1986) and in basal strata within the Havallah basin (Miller et al., 1984, 1992). Placing the mid-Paleozoic northern Sierran arc directly outboard of the Havallah basin also provides a source for influx of significant amounts of arc-type volcaniclastic debris that was shed from the west in the early Mississippian (Kinderhookian) into parts of the Havallah basin (Miller et al., 1984, 1992; Harwood and Murchey, 1990; Whiteford, 1990).

We know of no evidence requiring that strata in the lower three structural panels in the Shoo Fly Complex were already imbricated by thrusting prior to their southward transport along the western Laurentian margin. In contrast to

Colpron and Nelson (2009), we infer that west-vergent thrusting of Shoo Fly strata occurred in the accretionary complex associated with the west-facing Devonian northern Sierran arc, along with formation and thrust emplacement of the Sierra City mélange in the growing forearc complex. This interpretation is supported by evidence that some sediment masses within the mélange were mixed together prior to lithification and were still poorly consolidated when Late Devonian hypabyssal intrusions were injected into them (Girty and Pardini, 1987; Mount, 1990); it is also consistent with the fact that limited numbers of zircons from sandstone blocks within the mélange have yielded U-Pb ages as young as Late Devonian, although as noted above, additional work is needed to clarify the significance of these data.

Ediacaran tonalite blocks and detrital zircons with non–western Laurentian age spectra in the Sierra City mélange still must be explained. We suggest that this material was derived from a continuation of the Yreka and Trinity terranes within the eastern Klamath Mountains, or smaller terranes related to them that are no longer preserved, which were in close proximity to the developing Late Devonian northern Sierran arc. This interpretation is consistent with the presence of closely similar faunal assemblages in limestone blocks (Potter et al., 1990), similarities in detrital zircon populations in sandstone blocks, and tonalite blocks with Ediacaran zircon ages in both the Sierra City mélange and the Yreka terrane (Grove et al., 2008). Ediacaran tonalites also occur in the Trinity terrane (Wallin et al., 1988; Lindsley-Griffin et al., 2008). Possibly, parts of these older convergent margin assemblages were tectonically juxtaposed with the developing Late Devonian subduction complex in the Northern Sierra terrane and were incorporated into the younger subduction zone. Ordovician to Early Devonian zircons found in two sandstone blocks in the Sierra City mélange (Grove et al., 2008; this paper) also could have been derived from parts of the Yreka and Trinity terranes and the Lower to Middle Devonian arc sequence in the Redding section in the eastern Klamath Mountains, which contain detrital zircons or record igneous activity in the same time frame (Dickinson, 2000; Grove et al., 2008; Lindsley-Griffin et al., 2008). However, the starved-basin hemipelagic Upper Mississippian–Upper Pennsylvanian deposits of the upper Peale Formation in the Northern Sierra terrane show little similarity with age-equivalent strata in the Redding section, which record Late Devonian(?) to middle Mississippian clastic input followed by Pennsylvanian arc magmatism (Watkins, 1990). This suggests the two terranes became separated after the Early to Middle Devonian, although the histories of the two terranes converged in the mid-Permian, when they both became part of the McCloud arc festoon (Miller, 1987) and were then accreted to western Laurentia during the Sonoma orogeny.

It should be remembered that the present relative positions of the Northern Sierra terrane and the Yreka and Trinity terranes and Redding section in the eastern Klamath Mountains are the result of a long series of tectonic events that transpired following the early to mid-Paleozoic convergent margin tectonism recorded within them. Because Permian strata within these terranes contain the McCloud fauna, they must have migrated far into the ancestral northeast Pacific as the Slide Mountain ocean progressively opened. The terranes must then have migrated back to the western Laurentian margin as that ocean closed in order to become involved in the Permian–Triassic Sonoma orogeny and were subsequently displaced again during Mesozoic and Cenozoic tectonism, as described by Dickinson (2006). Thus, the present spatial arrangement of the Northern Sierra terrane and the eastern Klamath terranes may have little bearing on their original relative positions in the Late Devonian. Perhaps the presence of tonalite blocks and detrital zircons in sandstone blocks in the Sierra City mélange in the Northern Sierra terrane having similar non–western Laurentian age signatures to Early Devonian and older units in the eastern Klamath terranes provides an important clue as to their spatial relations prior to opening of the Slide Mountain ocean.

ACKNOWLEDGMENTS

We would like to express our gratitude to the following: Marty Grove and Elizabeth Miller (Stanford) for their invaluable help at all stages of this research; U.S. Geological Survey–Stanford SHRIMP-RG personnel and especially Matt Coble for his help with facilities; Trevor Dumitru (Stanford) for his help with the mineral separation; Kelley Brumley and Kris Meisling (all from Stanford) for useful discussion; Joan Kimbrough (San Diego State University) for her assistance with the use of X-ray fluorescence facilities; Pablo Garcia del Real, Sergei Nikolaev (deceased), Dmitry Malyshev, David Boinagrov, Nikita Powerman, and Helge Asleben (Texas Christian University) for their help in the field; and Doug Peterman from Downieville, California, for generously allowing us to pass through his property in the field. We are grateful to editors David Fastovsky and Christopher Spencer as well as Luke Beranek and two anonymous reviewers for substantially improving the manuscript. This work was possible due to the funding from the State Assignment of the Institute of Physics of the Earth, Russian Academy of Sciences, task 0144–2014–0091. Research was carried out of in frame Project #39 of the Program of Fundamental Research of SB RAS "interdisciplinary integration research" for 2018—2020.

REFERENCES CITED

Anderson, T.B., Woodard, G.D., Strathouse, S.M., and Twichell, M.K., 1974, Geology of a Late Devonian fossil locality in the Sierra Buttes Formation, Dugan Pond, Sierra City quadrangle, California [abs.]: Geological Society of America Abstracts with Programs, v. 6, no. 3, p. 139.

Anfinson, O.A., Leier, A.L., Embry, A.F., and Dewing, K., 2011, Detrital zircon geochronology and provenance of the Neoproterozoic to Late Devonian Franklinian Basin, Canadian Arctic Islands: Geological Society of America Bulletin, v. 124, p. 415–430, https://doi.org/10.1130/B30503.1.

Bacon, C.R., 1986, Magmatic inclusions in silicic and intermediate volcanic rocks: Journal of Geophysical Research, v. 91, p. 6091–6112, https://doi.org/10.1029/JB091iB06p06091.

Barbarin, B., 2005, Mafic magmatic enclaves and mafic rocks associated with some granitoids of the central Sierra Nevada Batholith, California: Nature, origin, and relations with the hosts: Lithos, v. 80, p. 155–177, https://doi.org/10.1016/j.lithos.2004.05.010.

Barth, A.P., and Wooden, J.L., 2010, Coupled elemental and isotopic analyses of polygenetic zircons from granitic rocks by ion microprobe, with implications for melt evolution and the sources of granitic magmas: Chemical Geology, v. 277, p. 149–159, https://doi.org/10.1016/j.chemgeo.2010.07.017.

Bateman, P.C., and Chappell, B.W., 1979, Crystallization, fractionation, and solidification of the Tuolumne intrusive series, Yosemite National Park, California: Geological Society of America Bulletin, v. 90, p. 465–482, https://doi.org/10.1130/0016-7606(1979)90<465:CFASOT>2.0.CO;2.

Bazard, D.R., Butler, R.F., Gehrels, G.E., and Soja, C.M., 1995, Paleomagnetism of the Early Devonian Karheen Formation, southeast Alaska: Implications for Alexander terrane paleogeography: Geology, v. 23, p. 707–710, https://doi.org/10.1130/0091-7613(1995)023<0707:EDPDFT>2.3.CO;2.

Belasky, P., Stevens, C.H., and Hanger, R.A., 2002, Early Permian location of western North American terranes based on brachiopod, fusulinid and coral biogeography: Palaeogeography, Palaeoclimatology, Palaeoecology, v. 179, p. 245–266, https://doi.org/10.1016/S0031-0182(01)00437-0.

Beranek, L.P., van Staal, C.R., McClelland, W.C., Israel, S., and Mihalynuk, M.G., 2013, Baltican crustal provenance for Cambrian–Ordovician sandstones of the Alexander terrane, North American Cordillera: Evidence from detrital zircon U-Pb geochronology and Hf isotope geochemistry: Journal of the Geological Society [London], v. 170, p. 7–18, https://doi.org/10.1144/jgs2012-028.

Beranek, L.P., Link, P.K., and Fanning, C.M., 2016, Detrital zircon record of mid-Paleozoic convergent margin activity in the northern U.S. Rocky Mountains: Implications for the Antler orogeny and early evolution of the North American Cordillera: Lithosphere, v. 8, p. 533–550, https://doi.org/10.1130/L557.1.

Black, L.P., Kamo, S.L., Allen, C.M., Davis, D.W., Aleinikoff, J.N., Valley, J.W., Mundil, R., Campbell, I.H., Korsch, R.J., Williams, I.S., and Foudoulis, C., 2004, Improved $^{206}Pb/^{238}U$ microprobe geochronology by the monitoring of a trace-element–related matrix effect; SHRIMP, ID-TIMS, ELA-ICP-MS and oxygen isotope documentation for a series of zircon standards: Chemical Geology, v. 205, no. 1–2, p. 115–140, https://doi.org/10.1016/j.chemgeo.2004.01.003.

Blake, D.H., Elwell, R.W.D., Gibson, I.L., Skelhorn, R.R., and Walker, G.P.L., 1965, Some relationships resulting from the intimate association of acid and basic magmas: Quarterly Journal of the Geological Society of London, v. 121, p. 31–49, https://doi.org/10.1144/gsjgs.121.1.0031.

Brooks, E.R., 2000, Geology of a late Paleozoic island arc in the Northern Sierra terrane, *in* Brooks, E.R., and Dida, L.T., eds., Field Guide to the Geology and Tectonics of the Northern Sierra Nevada: National Association of Geoscience Teachers, Far-Western Section, Special Publication 122, p. 53–110.

Brooks, E.R., and Coles, D.G., 1980, Use of immobile trace elements to determine original tectonic setting of eruption of metabasalts, northern Sierra Nevada, California: Geological Society of America Bulletin, v. 91, p. 665–671, https://doi.org/10.1130/0016-7606(1980)91<665:UOITET>2.0.CO;2.

Brown, E.H., Gehrels, G.E., and Valencia, V.A., 2010, Chilliwack composite terrane in northwest Washington: Neoproterozoic–Silurian passive margin basement, Ordovician–Silurian arc inception: Canadian Journal of Earth Sciences, v. 47, p. 1347–1366, https://doi.org/10.1139/E10-047.

Burchfiel, B.C., and Royden, L.H., 1991, Antler orogeny: A Mediterranean-type orogeny: Geology, v. 19, no. 1, p. 66–69, https://doi.org/10.1130/0091-7613(1991)019<0066:AOAMTO>2.3.CO;2.

Butler, R.F., Gehrels, G.E., and Bazard, D.R., 1997, Paleomagnetism of Paleozoic strata of the Alexander terrane, southeastern Alaska: Geological Society of America Bulletin, v. 109, p. 1372–1388, https://doi.org/10.1130/0016-7606(1997)109<1372:POPSOT>2.3.CO;2.

Cecil, M.R., Rotberg, G.L., Ducea, M.N., Saleeby, J.B., and Gehrels, G.E., 2012, Magmatic growth and batholithic root development in the northern Sierra Nevada, California: Geosphere, v. 8, p. 592–606, https://doi.org/10.1130/GES00729.1.

Coleman, D.S., Gray, W., and Glazner, A.F., 2004, Rethinking the emplacement and evolution of zoned plutons: Geochronologic evidence for incremental assembly of the Tuolumne intrusive suite: California Geology, v. 32, no. 5, p. 433–436, https://doi.org/10.1130/G20220.1.

Colpron, M., and Nelson, J.L., 2009, A Palaeozoic Northwest Passage: Incursion of Caledonian, Baltican and Siberian terranes into eastern Panthalassa, and the early evolution of the North American Cordillera: Geological Society [London] Special Publication 318, p. 273–307, https://doi.org/10.1144/SP318.10.

Colpron, M., and Nelson, J., 2011, A Palaeozoic NW Passage and the Timanian, Caledonian and Uralian connections of some exotic terranes in the North American Cordillera, *in* Spencer, A.M., Embry, A.F., Gautier, D.L., Stoupakova, A.V., and Sørensen, K., eds., Arctic Petroleum Geology: Geological Society [London] Memoir 35, p. 463–484, https://doi.org/10.1144/M35.31.

d'Allura, J.A., Moores, E.M., and Robinson, L., 1977, Paleozoic rocks of the northern Sierra Nevada: Their structural and paleogeographic implications, *in* Stewart, J.H., et al., eds., Paleozoic Paleogeography of the Western United States: Los Angeles, California, Pacific Section, Society of Economic Paleontologists and Mineralogists (SEPM), Pacific Coast Paleogeography Symposium 1, p. 395–408.

Davis, J.W., Coleman, D.S., Gracely, J.T., Gaschnig, R., and Stearns, M., 2012, Magma accumulation rates and thermal histories of plutons of the Sierra Nevada batholith, CA: Contributions to Mineralogy and Petrology, v. 163, no. 3, p. 449–465, https://doi.org/10.1007/s00410-011-0683-7.

Dickinson, W.R., 2000, Geodynamic interpretation of Paleozoic tectonic trends oriented oblique to the Mesozoic Klamath-Sierran continental margin in California, *in* Soreghan, M.J., and Gehrels, G.E., eds., Paleozoic and Triassic Paleogeography and Tectonics of Western Nevada and Northern California: Geological Society of America Special Paper 347, p. 209–245, https://doi.org/10.1130/0-8137-2347-7.209.

Dickinson, W.R., 2006, Geotectonic evolution of the Great Basin: Geosphere, v. 2, p. 353–368, https://doi.org/10.1130/GES00054.1.

Dusel-Bacon, C., Hopkins, M.J., Mortensen, J.K., Dashevsky, S.S., Bressler, J.R., Day, W.C., Colpron, M., and Nelson, J.L., 2006, Paleozoic tectonic and metallogenic evolution of the pericratonic rocks of east-central Alaska and adjacent Yukon, *in* Colpron, M., and Nelson, J.L., eds., Paleozoic Evolution and Metallogeny of Pericratonic Terranes at the Ancient Pacific Margin of North America, Canadian and Alaskan Cordillera: Geological Association of Canada Special Paper 45, p. 25–74.

Frazer, R.E., Coleman, D.S., and Mills, R.D., 2014, Zircon U-Pb geochronology of the Mount Givens Granodiorite: Implications for the genesis of large volumes of eruptible magma: Journal of Geophysical Research–Solid Earth, v. 119, p. 2907–2924, https://doi.org/10.1002/2013JB010716.

Frost, B.R., and Frost, C.D., 2008, A geochemical classification for feldspathic igneous rocks: Journal of Petrology, v. 49, p. 1955–1969, https://doi.org/10.1093/petrology/egn054.

Frost, B.R., Barnes, C.G., Collins, W.J., Arculus, R.J., Ellis, D.J., and Frost, C.D., 2001, A geochemical classification for granitic rocks: Journal of Petrology, v. 42, p. 2033–2048, https://doi.org/10.1093/petrology/42.11.2033.

Frost, T.P., and Mahood, G.A., 1987, Field, chemical, and physical constraints on mafic-felsic magma interaction in the Lamarck Granodiorite, Sierra Nevada, California: Geological Society of America Bulletin, v. 99, p. 272–291, https://doi.org/10.1130/0016-7606(1987)99<272:FCAPCO>2.0.CO;2.

Gehrels, G., and Pecha, M., 2014, Detrital zircon U-Pb geochronology and Hf isotope geochemistry of Paleozoic and Triassic passive margin strata of western North America: Geosphere, v. 10, p. 49–65, https://doi.org/10.1130/GES00889.1.

Girty, G.H., and Pardini, C.H., 1987, Provenance of sandstone inclusions in the Paleozoic Sierra City mélange, Sierra Nevada, California: Geological Society of America Bulletin, v. 98, p. 176–181, https://doi.org/10.1130/0016-7606(1987)98<176:POSIIT>2.0.CO;2.

Girty, G.H., and Wardlaw, M.S., 1984, Was the Alexander terrane a source of feldspathic sandstones in the Shoo Fly Complex, Sierra Nevada, California?: Geology, v. 12, p. 339–342, https://doi.org/10.1130/0091-7613(1984)12<339:WTATAS>2.0.CO;2.

Girty, G.H., Wardlaw, M.S., Schweickert, R.A., Hanson, R.E., and Bowring, S.A., 1984, Timing of pre-Antler deformation in the Shoo Fly Complex, Sierra Nevada, California: Geology, v. 12, p. 673–676, https://doi.org/10.1130/0091-7613(1984)12<673:TOPDIT>2.0.CO;2.

Girty, G.H., Gesster, K.C., and Turner, J.B., 1990, Pre–Late Devonian geochemical, stratigraphic, sedimentologic, and structural patterns, Shoo Fly complex, northern Sierra Nevada, California, *in* Harwood, D.S., and Miller, M.M., eds., Paleozoic and Early Mesozoic Paleogeographic Relations, Sierra Nevada, Klamath Mountains, and Related Terranes: Geological Society of America Special Paper 255, p. 43–56, https://doi.org/10.1130/SPE255-p43.

Girty, G.H., Keller, A.M., Franklin, K.R., and Stroh, R.C., 1991, The southernmost lens of the Upper Devonian Grizzly Formation, northern Sierra Nevada, California: Evidence for a trench-slope depositional setting, *in* Cooper, J., and Stevens, C., eds., Paleozoic Paleogeography of the Western United States–II: Los Angeles, California, Pacific Section, Society of Economic Paleontologists and Mineralogists (SEPM), Book 67, p. 693–701.

Girty, G.H., Lawrence, J., Burke, T., Fortin, A., Gallarano, C.S., Wirths, T.A., Lewis, J.G., Peterson, M.M., Ridge, D.L., Knaack, C., and Johnson, D., 1996, The Shoo Fly complex: Its origin and tectonic significance, *in* Girty, G.H., Hanson, R.E., Schweickert, R.A., and Harwood, D.S., eds., The Northern Sierra Terrane and Associated Mesozoic Magmatic Units: Implications for the Tectonic History of the Western Cordillera: Los Angeles, California, Pacific Section, Society of Economic Paleontologists and Mineralogists (SEPM), Book 81, p. 1–24.

Glazner, A.F., Bartley, J.M., Coleman, D.S., Gray, W., and Taylor, R.Z., 2004, Are plutons assembled over millions of years by amalgamation from small magma chambers?: GSA Today, v. 14, no. 4, p. 4–11, https://doi.org/10.1130/1052-5173(2004)014<0004:APAOMO>2.0.CO;2.

Goebel, K.A., 1991. Paleogeographic setting of Late Devonian to Early Mississippian transition from passive to collisional margin, Antler foreland, eastern Nevada and western Utah, *in* Cooper, J.D., and Stevens, C.H., eds., Paleozoic paleogeography of the Western United States II: Pacific Section, Society of Economic Paleontologists and Mineralogists, v. 67, p. 401–418.

Gradstein, F.M., and Ogg, J.G., 2012, The Chronostratigraphic Scale, *in* Gradstein, F.M., Ogg, J.G., and Schmitz, M., eds., 2012, The Geologic Time Scale 2012: Oxford, UK, Elsevier, v. 1, p. 31–24.

Grove, M.J., Gehrels, G.E., Cotkin, S.J., Wright, J.E., and Zou, H., 2008, Non-Laurentian cratonal provenance of Late Ordovician eastern Klamath blueschists and a link to the Alexander terrane, *in* Wright, J.E., and Shervais, J.W., eds., Ophiolites, Arcs, and Batholiths: A Tribute to Cliff Hopson: Geological Society of America Special Paper 438, p. 223–250, https://doi.org/10.1130/2008.2438(08).

Hannah, J.L., and Moores, E.M., 1986, Age relationships and depositional environments of Paleozoic strata, northern Sierra Nevada, California: Geological Society of America Bulletin, v. 97, p. 787–797, https://doi.org/10.1130/0016-7606(1986)97<787:ARADEO>2.0.CO;2.

Hanson, R.E., 1983, Volcanism, Plutonism and Sedimentation in a Late Devonian Submarine Island-Arc Setting, Northern Sierra Nevada, California [Ph.D. dissertation]: New York, Columbia University, 345 p.

Hanson, R.E., 1991, Quenching and hydroclastic disruption of andesitic to rhyolitic intrusions in a submarine island-arc sequence, northern Sierra Nevada, California: Geological Society of America Bulletin, v. 103, p. 804–816, https://doi.org/10.1130/0016-7606(1991)103<0804:QAHDOA>2.3.CO;2.

Hanson, R.E., and Schweickert, R.A., 1982, Chilling and brecciation of a Devonian rhyolite sill intruded into wet sediments, northern Sierra Nevada, California: The Journal of Geology, v. 90, p. 717–724, https://doi.org/10.1086/628726.

Hanson, R.E., and Schweickert, R.A., 1986, Stratigraphy of mid-Paleozoic island-arc rocks in part of the northern Sierra Nevada, Sierra and Nevada Counties, California: Geological Society of America Bulletin, v. 97, p. 986–998, https://doi.org/10.1130/0016-7606(1986)97<986:SOMIRI>2.0.CO;2.

Hanson, R.E., Saleeby, J.B., and Schweickert, R.A., 1988, Composite Devonian island-arc batholith in the northern Sierra Nevada, California: Geological Society of America Bulletin, v. 100, p. 446–457, https://doi.org/10.1130/0016-7606(1988)100<0446:CDIABI>2.3.CO;2.

Hanson, R.E., Girty, G.H., Girty, M.S., Hargrove, U.S., Harwood, D.S., Kulow, M.J., Mielke, K.L., Phillipson, S.E., Schweickert, R.A., and Templeton, J.H., 1996, Paleozoic and Mesozoic arc rocks in the northern Sierra terrane, *in* Girty, G.H., Hanson, R.E., Harwood, D.S., and Schweickert, R.A., eds., The Northern Sierra Terrane and Associated Mesozoic Magmatic Units: Implications for the Tectonic History of the Western Cordillera: Los Angeles, California, Pacific Section, Society for Sedimentary Geology (SEPM), Book 81, p. 25–55.

Hanson, R.E., Girty, G.H., Harwood, D.S., and Schweickert, R.A., 2000, Paleozoic subduction complex and Paleozoic–Mesozoic island-arc volcano-plutonic assemblages in the northern Sierra terrane, *in* Lageson, D.R., Peters, S.G., and Lahren, M.M., eds., Great Basin and Sierra Nevada: Geological Society of America Field Guide 2, p. 255–277, https://doi.org/10.1130/0-8137-0002-7.255.

Harding, J.P., Gehrels, G.E., Harwood, D.S., and Girty, G.H., 2000, Detrital zircon geochronology of the Shoo Fly Complex, northern Sierra terrane, northeastern California, *in* Soreghan, M.J., and Gehrels, G.E., eds., Paleozoic and Triassic Paleogeography and Tectonics of Western Nevada and Northern California: Geological Society of America Special Paper 347, p. 43–55, https://doi.org/10.1130/0-8137-2347-7.43.

Harwood, D.S., 1992, Stratigraphy of Paleozoic and Lower Mesozoic Rocks in the Northern Sierra Terrane, California: U.S. Geological Society of America Bulletin 1957, 78 p.

Harwood, D.S., and Murchey, B.L., 1990, Biostratigraphic, tectonic, and paleogeographic ties between Upper Paleozoic volcanic and basinal rocks in the northern Sierra terrane, California, and the Havallah sequence, Nevada, *in* Harwood, D.S., and Miller, M.M., eds., Paleozoic and Early Mesozoic Paleogeographic Relations: Sierra Nevada, Klamath Mountains, and Related Terranes: Geological Society of America Special Paper 255, p. 157–174, https://doi.org/10.1130/SPE255-p157.

Linde, G.M., Trexler, J.H., Jr., Cashman, P.H., Gehrels, G., and Dickinson, W.R., 2016, Detrital zircon U-Pb geochronology and Hf isotope geochemistry of the Roberts Mountains allochthon: New insights into the early Paleozoic tectonics of western North America: Geosphere, v. 12, p. 1016–1031, https://doi.org/10.1130/GES01252.1.

Linde, G.M., Trexler, J.H., Cashman, P.H., Gehrels, G., and Dickinson, W.R., 2017, Three-dimensional evolution of the early Paleozoic western Laurentian margin: New insights from detrital zircon U-Pb geochronology and Hf isotope geochemistry of the Harmony Formation of Nevada: Tectonics, v. 36, p. 2347–2369, https://doi.org/10.1002/2017TC004520.

Lindsley-Griffin, N., Griffin, J.R., and Farmer, J.D., 2008, Paleogeographic significance of Ediacaran cyclomedusoids within the Antelope Mountain Quartzite, Yreka subterrane, eastern Klamath Mountains, California, *in* Blodgett, R.B., and Stanley, G.D., Jr., eds., The Terrane Puzzle: New Perspectives on Paleontology and Stratigraphy from the North American Cordillera: Geological Society of America Special Paper 442, p. 1–37, https://doi.org/10.1130/2008.442(01).

Ludwig, K.R., 2003, User's Manual for Isoplot 3.00: A Geochronological Toolkit for Microsoft Excel: Berkeley Geochronology Center Special Publication 4, 73 p.

Ludwig, K.R., 2009, SQUID 2: A User's Manual, Rev. 12 April 2009: Berkeley Geochronology Center Special Publication 5, 110 p.

Mahon, K.I., 1996, The New "York" regression: Application of an improved statistical method to geochemistry: International Geology Review, v. 38, p. 293–303, https://doi.org/10.1080/00206819709465336.

Mattinson, J.M., 2010, Analysis of the relative decay constants of ^{235}U and ^{238}U by multi-step CA-TIMS measurements of closed-system natural zircon samples: Chemical Geology, v. 275, no. 3–4, p. 186–198, https://doi.org/10.1016/j.chemgeo.2010.05.007.

Menand, T., Annen, C., and de Saint Blanquat, M., 2015, Rates of magma transfer in the crust: Insights into magma reservoir recharge and pluton growth: Geology, v. 43, p. 199–202, https://doi.org/10.1130/G36224.1.

Middlemost, E.A.K., 1994, Naming materials in the magma igneous rock system: Earth-Science Reviews, v. 37, p. 215–224, https://doi.org/10.1016/0012-8252(94)90029-9.

Miller, E.L., Holdsworth, B.K., Whiteford, W.B. and Rodgers, D., 1984, Stratigraphy and structure of the Schoonover sequence, northeastern Nevada: Implications for Paleozoic plate-margin tectonics. Geological Society of America Bulletin, v. 95, p.1063–1076, https://doi.org/10.1130/0016-7606(1984)95<1063:SASOTS>2.0.CO;2.

Miller, E.L., Miller, M.M., Stevens, C.H., Wright, J.E. and Madrid, R., 1992, Late Paleozoic paleogeographic and tectonic evolution of the western US cordillera, *in* Burchfiel, B.C., Lipman, P.W., and Zoback, M.L., eds., The Cordilleran Orogen: Conterminous U.S.: Geological Society of America, The Geology of North America, v. G-3, p. 57–106, https://doi.org/10.1130/DNAG-GNA-G3.57.

Miller, E.L., Kuznetsov, N.B., Soboleva, A.A., Udoratina, O.V., Grove, M.J., and Gehrels, G.E., 2011, Baltica in the Cordillera?: Geology, v. 39, p. 791–794, https://doi.org/10.1130/G31910.1.

Miller, M.M., 1987, Dispersed remnants of a northeast Pacific fringing arc: Upper Paleozoic terranes of Permian McCloud faunal affinity, western US: Tectonics, v. 6, no. 6, p. 807–830, https://doi.org/10.1029/TC006i006p00807.

Monger, J.W.H., Struik, L.C., Haggart, J.W., and Enkin, R.J., 2006, Chilliwack terrane: A slice of Stikinia?: A tale of terrane transfer, *in* Haggart, J.W., Enkin, R.J., and Monger, J.W.H., eds., Paleogeography of the North American Cordillera: Evidence For and Against Large-Scale Displacements: Geological Association of Canada Special Paper 46, p. 351–368.

Mount, C.M., 1990, Geology of the Sierra City Mélange Unit of the Shoo Fly Complex in the Lakes Basin Region, Northern Sierra Nevada, California [M.S. thesis]: Reno, Nevada, University of Nevada, 86 p.

Mount, C.M., and Schweickert, R.A., 1986, Paleozoic orogeny in the Shoo Fly: Evidence from clastic rocks in the Sierra City mélange, California: Geological Society of America Abstracts with Programs, v. 18, p. 162.

Nelson, J.L., Colpron, M., and Israel, S., 2013, The Cordillera of British Columbia, Yukon, and Alaska: Tectonics and metallogeny, *in* Colpron, M., Bissig, T., Rusk, B.G., and Thompson, J.F.H., eds., Tectonics, Metallogeny, and Discovery: The North American Cordillera and Similar Accretionary Settings: Society of Economic Geologists Special Publication 17, p. 53–109.

Paces, J.B., and Miller, J.D., 1993, Precise U-Pb ages of Duluth Complex and related mafic intrusions, northeastern Minnesota: Geochronological insights to physical, petrogenetic, paleomagnetic, and tectonomagmatic processes associated with the 1.1 Ga Midcontinent Rift system: Journal of Geophysical Research, v. 98, p. 13,997–14,013, https://doi.org/10.1029/93JB01159.

Paradis, S., Bailey, S.L., Creaser, R.A., Piercey, S.J., Schiarizza, P., Colpron, M., and Nelson, J.L., 2006, Paleozoic magmatism and syngenetic massive sulphide deposits of the Eagle Bay assemblage, Kootenay terrane, southern British Columbia, *in* Colpron, M., and Nelson, J.L., eds., Paleozoic Evolution and Metallogeny of Pericratonic Terranes at the Ancient Pacific Margin of North America, Canadian and Alaskan Cordillera: Geological Association of Canada Special Paper 45, p. 383–414.

Paton, C., Hellstrom, J., Paul, B., Woodhead, J., and Hergt, J., 2011, Iolite: Freeware for the visualisation and processing of mass spectrometric data: Journal of Analytical Atomic Spectrometry, v. 26, p. 2508–2518, https://doi.org/10.1039/c1ja10172b.

Pearce, J.A., 1982. Trace element characteristics of lavas from destructive plate boundaries, *in* Thorpe, R.S., ed., Andesites: Orogenic Andesites and Related Rocks: Chichester, UK, John Wiley and Sons, p. 525–548.

Pearce, J.A., Harris, N.B.W., and Tindle, A.G., 1984, Trace element distribution diagrams for the tectonic interpretation of granitic rocks: Journal of Petrology, v. 25, p. 956–983, https://doi.org/10.1093/petrology/25.4.956.

Pecha, M.E., Gehrels, G.E., McClelland, W.C., Giesler, D., White, C., and Yokelson, I., 2016, Detrital zircon U-Pb geochronology and Hf isotope geochemistry of the Yukon-Tanana terrane, Coast Mountains, southeast Alaska: Geosphere, v. 12, p. 1556–1574, https://doi.org/10.1130/GES01303.1.

Petford, N., Cruden, A.R., McCaffrey, K.J.W., and Vigneresse, J.L., 2000, Granite magma formation, transport and emplacement in the Earth's crust: Nature, v. 408, p. 669–673, https://doi.org/10.1038/35047000.

Piercey, S.J., Murphy, D.C., and Creaser, R.A., 2012, Lithosphere-asthenosphere mixing in a transform-dominated late Paleozoic backarc basin: Implications for northern Cordilleran crustal growth and assembly: Geosphere, v. 8, p. 716–739, https://doi.org/10.1130/GES00757.1.

Potter, A.W., Watkins, R., Boucot, A.J., Elias, R.J., Flory, R.A., and Rigby, J.K., 1990, Biogeography of the Upper Ordovician Montgomery limestone, Shoo Fly Complex, northern Sierra Nevada, California, and comparisons of the Shoo Fly Complex with the Yreka terrane, *in* Harwood, D.S., and Miller, M.M., eds., Paleozoic and Early Mesozoic Paleogeographic Relations: Sierra Nevada, Klamath Mountains, and Related Terranes: Geological Society of America Special Paper 255, p. 33–42, https://doi.org/10.1130/SPE255-p33.

Powerman, V.I., Buyantuev, M.D., and Ivanov, A.V., 2018, Dezirteer—Software for a rapid analysis and filtering of U-Pb data, reduced in Glitter or Iolite, *in* Proceedings of the Conference "Geodynamic Evolution of the Central-Asian Mobile Belt (from Ocean to Continent)": Irkutsk, Russia, Institute of Earth's Crust, Siberian Branch, Russian Academy of Sciences, p. 199–200.

Rollinson, H., 1993, Using Geochemical Data: Evaluation, Presentation, Interpretation: Harlow, UK, Longman Scientific & Technical, 352 p.

Rouer, O., Lapierre, H., and Coulon, C., 1988, La série calco-alcaline permienne d'arc du N de la Sierra Nevada (California, U.S.A.): Ultime étape magmatique dans l'évolution de la bordure de la microplaque Sonomia: Comptes Rendus de l'Académie des Sciences, ser. II, v. 307, p. 57–62.

Rouer, O., Lapierre, H., Coulon, C., and Michard, A., 1989, New petrological and geochemical data on mid-Paleozoic island-arc volcanics of northern Sierra Nevada, California: Evidence for a continent-based island arc: Canadian Journal of Earth Sciences, v. 26, p. 2465–2478, https://doi.org/10.1139/e89-210.

Rubin, C.M., Miller, M.M., and Smith, G.M., 1990, Tectonic development of Cordilleran mid-Paleozoic volcano-plutonic complexes: Evidence for convergent margin tectonism, *in* Harwood, D.S., and Miller, M.M., eds., Paleozoic and Early Mesozoic Paleogeographic Relations: Sierra Nevada, Klamath Mountains, and Related Terranes: Geological Society of America Special Paper 255, p. 1–16, https://doi.org/10.1130/SPE255-p1.

Saleeby, J., 1990, Geochronological and tectonostratigraphic framework of Sierran-Klamath ophiolitic assemblages, *in* Harwood, D.S., and Miller, M.M., eds., Paleozoic and Early Mesozoic Paleogeographic Relations: Sierra Nevada, Klamath Mountains, and Related Terranes: Geological Society of America Special Paper 255, p. 93–114, https://doi.org/10.1130/SPE255-p93.

Saleeby, J.B., Hannah, J.L., and Varga, R.J., 1987, Isotopic age constraints on middle Paleozoic deformation in the Northern Sierra Nevada, California: Geology, v. 15, p. 757–760, https://doi.org/10.1130/0091-7613(1987)15<757:IACOMP>2.0.CO;2.

Saleeby, J., Shaw, H.F., Moores, E.M., and Edelman, S.H., 1989, U/Pb, Sm/ Nd, and Rb/Sr geochronological and isotopic study of northern Sierra Nevada ophiolitic assemblages: Contributions to Mineralogy and Petrology, v. 102, p. 205–220, https://doi.org/10.1007/BF00375341.

Saucedo, G.J., and Wagner, D.L., 1992, Geologic Map of the Chico Quadrangle, California: California Division of Mines and Geology Regional Geologic Map 7A, scale 1:250,000.

Schellart, W.P., Freeman, J., Stegman, D.R., Moresi, L., and May, D., 2007, Evolution and diversity of subduction zones controlled by slab width: Nature, v. 446, p. 308, https://doi.org/10.1038/nature05615.

Schermer, E.R., Hoffnagle, E.A., Brown, E.H., Gehrels, G.E., and McClelland, W.C., 2018, U-Pb and Hf isotopic evidence for an Arctic origin of terranes in northwestern Washington: Geosphere, v. 14, p. 835–860, https://doi.org/10.1130/GES01557.1.

Schoene, B., 2014, U-Th-Pb geochronology, *in* Holland, H.D., and Turekian, K.K., eds., Treatise on Geochemistry Volume 4: The Crust: Oxford, UK, Elsevier, p. 341–378, https://doi.org/10.1016/B978-0-08-095975-7.00310-7.

Schweickert, R.A., 2015, Jurassic evolution of the Western Sierra Nevada metamorphic province, *in* Anderson, T.H., Didenko, A.N., Johnson, C.L., Khanchuk, A.I., and MacDonald, J.H., Jr., eds., Late Jurassic Margin of Laurasia—A Record of Faulting Accommodating Plate Rotation: Geological Society of America Special Paper 513, p. 299–358, https://doi.org/10.1130/2015.2513(08).

Schweickert, R.A., and Girty, G.H., 1981, Significance of the unconformity between Shoo Fly Complex and Paleozoic island-arc sequences, north Sierra Nevada, California: Geological Society of America Abstracts with Programs, v. 13, p. 105.

Schweickert, R.A., and Snyder, W.S., 1981, Paleozoic plate tectonics of the Sierra Nevada and adjacent regions, *in* Ernst, W.G., ed., The Geotectonic Development of California: Englewood Cliffs, New Jersey, Prentice-Hall, p. 182–210.

Schweickert, R.A., Harwood, D.S., Girty, G.H., and Hanson, R.E., 1984, Tectonic development of the northern Sierra terrane: An accreted late Paleozoic island arc and its basement (field trip 5), *in* Lintz, J.J., ed., Western Geological Excursions, Volume 4: Reno, Nevada, Department of Geological Sciences, Mackey School of Mines, p. 1–65.

Shand, S.J., 1943, Eruptive Rocks: Their Genesis, Composition, and Classification, with a Chapter on Meteorites: New York, J. Wiley & Sons, Inc., 360 p.

Shea, E.K., Miller, J.S., Miller, R.B., Bowring, S.A., and Sullivan, K.M., 2016, Growth and maturation of a mid- to shallow-crustal intrusive complex, North Cascades, Washington: Geosphere, v. 12, p. 1489–1516, https://doi.org/10.1130/GES01290.1.

Silva, S.R., Bullen, T.D., and Brooks, E.R., 2000, Devonian Sierra Buttes Formation in the Jamison Lake area: Involvement of ancient continental crust in magma genesis, *in* Brooks, E.R., and Dida, L.T., eds., Field Guide to the Geology and Tectonics of the Northern Sierra Nevada: National Association of Geoscience Teachers, Far-Western Section, Special Publication 122, p. 16–52.

Soja, C.M., 2008, Silurian-bearing terranes of Alaska, *in* Blodgett, R.B., and Stanley, G.D., Jr., eds., The Terrane Puzzle: New Perspectives on Paleontology and Stratigraphy from the North American Cordillera: Geological Society of America Special Paper 442, p. 39–50, https://doi.org/10.1130/2008.442(02).

Soja, C.M., and Antoshkina, A.I., 1997, Coeval development of Silurian stromatolite reefs in Alaska and the Ural Mountains: Implications for paleogeography of the Alexander terrane: Geology, v. 25, p. 539–542, https://doi.org/10.1130/0091-7613(1997)025<0539:CDOSSR>2.3.CO;2.

Soja, C.M., and Krutikov, L., 2008, Provenance, depositional setting, and tectonic implications of Silurian polymictic conglomerate in Alaska's Alexander terrane, *in* Blodgett, R.B., and Stanley, G.D., Jr., eds., The Terrane Puzzle: New Perspectives on Paleontology and Stratigraphy from the North American Cordillera: Geological Society of America Special Paper 442, p. 63–75, https://doi.org/10.1130/2008.442(04).

Stevens, C.H., and Belasky, P., 2009, Nature of Permian faunas in western North America: A key to the understanding of the history of allochthonous terranes, *in* Ferrari, D.M., and Guiseppi, A.R., eds., Geomorphology and Plate Tectonics: New York, Nova Science Publishers, p. 275–310.

Wallin, E.T., Mattinson, J.M., and Potter, A.W., 1988, Early Paleozoic magmatic events in the eastern Klamath Mountains, northern California: Geology, v. 16, p. 144–148, https://doi.org/10.1130/0091-7613(1988)016<0144:EPMEIT>2.3.CO;2.

Watkins, R., 1990, Carboniferous and Permian island-arc deposits of the eastern Klamath terrane, California, *in* Harwood, D.S., and Miller, M.M., eds., Paleozoic and Early Mesozoic Paleogeographic Relations: Sierra Nevada, Klamath Mountains, and Related Terranes: Geological Society of America Special Paper 255, p. 193–200, https://doi.org/10.1130/SPE255-p193.

White, C., Gehrels, G.E., Pecha, M., Giesler, D., Yokelson, I., McClelland, W.C., and Butler, R.F., 2016, U-Pb and Hf isotope analysis of detrital zircons from Paleozoic strata of the southern Alexander terrane (southeast Alaska): Lithosphere, v. 8, p. 83–96, https://doi.org/10.1130/L475.1.

Whiteford, W.B., 1990, Paleogeographic setting of the Schoonover sequence, Nevada, and implications for the late Paleozoic margin of western North America, *in* Harwood, D.S., and Miller, M.M., eds., Paleozoic and Early Mesozoic Paleogeographic Relations: Sierra Nevada, Klamath Mountains, and Related Terranes: Geological Society of America Special Paper 255, p. 115–136, https://doi.org/10.1130/SPE255-p115.

Winchester, J.A., and Floyd, P.A., 1977, Geochemical discrimination of different magma series and their differentiation products using immobile elements: Chemical Geology, v. 20, p. 325–343, https://doi.org/10.1016/0009-2541(77)90057-2.

Wright, J.E., and Wyld, S.J., 2006, Gondwanan, Iapetan, Cordilleran interactions: A geodynamic model for the Paleozoic tectonic evolution of the North American Cordillera, *in* Haggart, J.W., Enkin, R.J., and Monger, J.W.H., eds., Paleogeography of the North American Cordillera: Evidence For and Against Large-Scale Displacements: Geological Association of Canada Special Paper 46, p. 377–408.

Yokelson, I., Gehrels, G.E., Pecha, M., Giesler, D., White, C., and McClelland, W.C., 2015, U-Pb and Hf isotope analysis of detrital zircons from Mesozoic strata of the Gravina belt, southeast Alaska: Tectonics, v. 34, p. 2052–2066, https://doi.org/10.1002/2015TC003955.